INVESTIGATING EFFECTS OF LOW TEMPERATURE CHANGE ON CONCRETE USING ACOUSTIC EMISSION MONITORING

By

IGNATIUS VASANT

Bachelor of Science in Civil Engineering

Visvesvaraya Technological University

Belgaum, Karnataka - India

2013

Submitted to the Faculty of the
Graduate College of the
Oklahoma State University
in partial fulfillment of
the requirements for
the Degree of
MASTER OF SCIENCE
July, 2015

INVESTIGATING EFFECTS OF TEMPERATURE CHANGE ON CONCRETE USING ACOUSTIC EMISSION MONITORING

Thesis Approved:

Dr. Julie Ann Hartell

Thesis Adviser

Dr. M. Tyler Ley

Committee Member

Dr. Xiaoming Yang

Committee Member

ACKNOWLEDGEMENTS

I would like to express my gratitude to my supervisor, Dr. Julie Ann Hartell, whose expertise, understanding, and patience, added considerably to my graduate experience. I attribute the level of my Master's degree to her encouragement and effort and without her this thesis, too, would not have been completed or written. One simply could not wish for a better or friendlier supervisor.

In my daily work, I have been blessed with a friendly and cheerful group of fellow students. I would like to express my gratitude towards Ms. Meher Lalitha Mandavilli, Mr. Wassay Gulrez and Ms. Harishma Donthineni. Their support and care helped me overcome setbacks and stay focused on my graduate study. I greatly value their friendship and I deeply appreciate their belief in me.

Most importantly, none of this would have been possible without the love and patience of my family. My immediate family to whom this dissertation is dedicated to, has been a constant source of love, concern, support and strength all these years. I would like to express my heart-felt gratitude to my parents, Mr. Stanley Sathyaraj and Mrs. Caroline Vatsala Stanley and sister, Maria Sneha.

Name: IGNATIUS VASANT

Date of Degree: JULY, 2015

Title of Study: INVESTIGATING EFFECTS OF TEMPERATURE CHANGE ON CONCRETE USING ACOUSTIC EMISSION MONITORING

Major Field: CIVIL ENGINEERING

Abstract:

Concrete subjected to freeze- thaw cycles is one of the effects which deteriorate the concrete exposed to water in cold weather conditions. To evaluate the damages in concrete caused by freezing, it is necessary to understand the formation of ice in the pores. In this research, the performance of concrete exposed to freeze thaw cycles was monitored using acoustic emission techniques. The historical temperature data for Oklahoma City was analyzed for eleven years and the appropriate exposure regimen was selected. The concrete samples were subjected to freeze-thaw cycles with temperature varying between -6.4°C and 4°C and 60% RH. It was noticed that there were few AE event clusters recorded which did not follow any particular trend. More number of AE events are observed to be at the freezing and freezing hold phase which could be due to the water freezing in the voids and capillary pores. Hits are also observed to be in Thaw and thaw – hold phase, this can be attributed to the expansion of concrete. Most of the amplitudes and energies recorded were low; thus, indicating that significant damage may not have occurred.

TABLE OF CONTENTS

TABLE OF CONTENTS v

LIST OF FIGURES vii

LIST OF TABLES viii

Chapter 1 INTRODUCTION 1

Chapter 2 REVIEW OF LITERATURE 3

2.1 Air Entrainment and Freeze-thaw Durability 5

2.2 Experimental Evaluation of Freeze-Thaw Durability 5

2.2.1 Standard Evaluation Methods 5

2.2.2 Non-Destructive Evaluation Methods 6

2.2.3 Destructive Evaluation Methods 6

2.2.4 Acoustic Emission Methods 7

2.3 Overview of Acoustic emission Monitoring 9

2.3.1 Stress-Wave Propagation Theory 10

2.3.2 Acoustic Emission Technique 13

Chapter 3 EXPERIMENTAL METHODOLOGY 17

3.1 Sample Preparation 17

3.1.1 Materials 17

3.1.2 Casting 18

3.1.3 Sample Curing and Conditioning 20

3.2 Freeze-Thaw Exposure Regimen 20

3.2.1 Temperature Profile 20

3.1.1 Exposure Regimen 21

3.3 Acoustic Emission Monitoring Techniques 23

3.3.1 AE Hardware 24

3.3.2 AE Software 25
3.3.3 Background Noise 25
Chapter 4 Results and Discussion 27
4.1 Damage Analysis During Freezing Phase 28
4.1.1 Amplitude and Number of Hits 28
4.1.2 Energy and Number of Hits 30
4.2 Damage Analysis during Freeze-Hold Phase 33
4.2.1 Amplitude and number of hits 33
4.1.2 Energy and number of hits 35
4.3 Damage Analysis during Thawing Phase 38
4.3.1 Amplitude and number of hits 38
4.3.2 Energy and number of hits 40
4.2 Damage Analysis during Thaw-Hold Phase 43
4.4.1 Amplitude and number of hits 43
4.4.2 Energy and number of hits 45
Chapter 5 Conclusion 48
REFERENCES 49
APPENDICES 55
Figure 15: Temperature vs Amplitude graph for channel 1 and 2 (cylindrical specimen 1) 59
VITA 63

LIST OF FIGURES

Figure 1: Decreasing percent of strength with increasing cycles of freeze-thaw..... 7

Figure 2: AE vs Temperature Cycles..... 8

Figure 3: Particle motion related to wave mode propagation types through a solid medium:..... 11

a) Compressional wave, b) shear wave and c) Rayleigh wave. 11

Figure 4: Schematic representation of acoustic emission testing..... 14

Figure 5: Waveform Parameters of AE Signal 15

Figure 6: Samples placed in environmental chamber for exposure regimen 22

Figure 7: Single freeze – thaw cycle..... 23

Figure 8: Sensor glued to the specimen 23

Figure 9: Wide band sensors..... 24

Figure 10: 2/4/6 Amplifier..... 25

LIST OF TABLES

Table 1: Mix Design Sheet 18

Table 2: Fresh concrete properties 19

Table 3: Statistical analysis of Recorded Daily Low Temperature for the months of December, January and February (Coolest months of the year) 21

Table 4: Number of AE hits per amplitude range during freezing phase for cylindrical specimen 1, channel 1 and 2. 28

Table 5: Number of AE hits per amplitude range during freezing phase for cylindrical specimen 2, channel 3 and 4. 29

Table 6: Number of AE hits per amplitude range during freezing phase for prism specimen 3, channel 5 and 6. 29

Table 7: Number of AE hits per amplitude range during freezing phase for prism specimen 4, channel 7 and 8. 30

Table 8: Number of AE hits per energy range during freezing phase for cylindrical specimen 1, channel 1 and 2. 31

Table 9: Number of AE hits per energy range during freezing phase for cylindrical specimen 2, channel 3 and 4. 31

Table 10: Number of AE hits per energy range during freezing phase for prism specimen 3, channel 5 and 6. 32

Table 11: Number of AE hits per energy range during freezing phase for prism specimen 4, channel 7 and 8. 32

Table 12: Number of AE hits per amplitude range during freeze-hold phase for cylindrical specimen 1, channel 1 and 2. 33
Table 13: Number of AE hits per amplitude range during freeze-hold phase for cylindrical specimen 2, channel 3 and 4. 34
Table 14: Number of AE hits per amplitude range during freeze-hold phase for prism specimen 3, channel 5 and 6. 34
Table 15: Number of AE hits per amplitude range during freeze-hold phase for prism specimen 4, channel 7 and 8. 35
Table 16: Number of AE hits per energy range during freeze-hold phase for cylindrical specimen 1, channel 1 and 2. 36
Table 17: Number of AE hits per energy range during freeze-hold phase for cylindrical specimen 2, channel 3 and 4. 36
Table 18: Number of AE hits per energy range during freeze-hold phase for prism specimen 3, channel 5 and 6. 37
Table 19: Number of AE hits per energy range during freeze-hold phase for prism specimen 4, channel 7 and 8. 37
Table 20: Number of AE hits per amplitude range during thawing phase for cylindrical specimen 1, channel 1 and 2. 38
Table 21: Number of AE hits per amplitude range during thawing phase for cylindrical specimen 2, channel 3 and 4. 39
Table 22: Number of AE hits per amplitude range during thawing phase for prism specimen 3, channel 5 and 6. 39

Table 23: Number of AE hits per amplitude range during thawing phase for prism specimen 4, channel 7 and 8. 40
Table 24: Number of AE hits per energy range during thawing phase for cylindrical specimen 1, channel 1 and 2. 41
Table 25: Number of AE hits per energy range during thawing phase for cylindrical specimen 2, channel 3 and 4. 41
Table 26: Number of AE hits per energy range during thawing phase for prism specimen 3, channel 5 and 6. 42
Table 27: Number of AE hits per energy range during thawing phase for prism specimen 4, channel 7 and 8. 42
Table 29: Number of AE hits per amplitude range during thaw-hold phase for cylindrical specimen 2, channel 3 and 4. 44
Table 30: Number of AE hits per amplitude range during thaw-hold phase for prism specimen 3, channel 5 and 6. 44
Table 31: Number of AE hits per amplitude range during thaw-hold phase for prism specimen 4, channel 7 and 8. 45
Table 32: Number of AE hits per energy range during thaw-hold phase for cylindrical specimen 1, channel 1 and 2. 46
Table 33: Number of AE hits per energy range during thaw-hold phase for cylindrical specimen 2, channel 3 and 4. 46
Table 34: Number of AE hits per energy range during thaw-hold phase for prism specimen 3, channel 5 and 6. 47

Table 35: Number of AE hits per energy range during thaw-hold phase for prism specimen 4, channel 7 and 8. 47

CHAPTER 1

INTRODUCTION

As the existing structures deteriorate, durability of concrete is of a major concern. For concrete structures in cold regions, durability of concrete for freeze-thaw is important. Freeze-thaw durability of concrete can be related to its pore structure. Various parameters such as radius, volume and pore size distribution govern the freezing point of pore solution and also the quantity of ice formed in these pores. Usually, within a particular temperature interval, more frozen pore solution induces higher internal hydraulic pressure which results in more severe frost damages.

"Thus the freezing point and the amount of frozen solution in pores reflect the frost durability of concrete" (Cai and Liu, 1998)

Frost action causes cracking and spalling of concrete which are the most common damages, and are caused due to progressive expansion of the cement paste by repeated freeze-thaw cycles. (Mehta and Monteiro 2006). Many theories were proposed to explain freeze-thaw damage, such as the osmotic pressure (Powers and Helmuth 1953), hydraulic pressure (Power TC 1958) and the micro-ice-lens model (Setzer 2001) are important among others. The frost damage is mainly studied in a laboratory by rapid freeze-thaw cycles. Several standards have been developed to evaluate the resistance of concrete subjected to accelerated freeze-thaw cycles. But, these standards differ in the testing techniques used and in the experimental methodology carried out for evaluating damage in

concrete. Concrete resistance to freeze-thaw damage is usually analyzed and categorized depending on the damage type, either external or internal. (Molero 2012)

In recent years, acoustic emission testing have been utilized to evaluate concrete deterioration mechanisms involving micro crack formation and propagation. It is an NDT technique that as initially developed more than five decades to test and monitor various types of metallic structures. It can be used to identify both the nature of the damage and the damage level. It gives information about the irreversible and real cracking processes in a material and, in more recent years, has been used for damage characterization of concrete structures (Shahidan et al. 2013).The damage in concrete may be characterized using AE parameters such as energy, amplitude, rise time and frequency.

In this study, the resistance of concrete to freezing and thawing cycles at temperatures representative of Oklahoman climate was evaluated using acoustic emission (AE) monitoring. A literature review of works was carried out and is detailed in Chapter 2. The latter served as the basis for the present research and helped in the development of the experimental methodology described in Chapter 3. This chapter elaborates on the methodology used to prepare the samples along with material information; the design of the temperature profiles and its experimental simulation; and the procedure and equipment used to monitor damage. Finally, the data obtained is analyzed and discussed in Chapter 4.

CHAPTER 2

REVIEW OF LITERATURE

Acoustic emission monitoring has been used over the past few decades to monitor the performance of concrete. Current use has been influenced by many works carried out in the past. This chapter provides an overview of past studies carried out on freeze – thaw mechanism of concrete and how acoustic emission technique can be used to monitor the performance of concrete subjected to freeze-thaw cycles.

Freeze-thaw durability of concrete is very important in cold areas. To evaluate the damage in concrete caused by freezing and thawing it is necessary to understand the process of ice formation in concrete pores. Cai and Liu (1998), demonstrated that freeze-thaw durability of concrete has a very close relationship with the concrete pore structure. The amount of ice formed in pores and the freezing point of pore solution depends on the volume, radius and size distribution of pores. Above -10°C, the freezing rate of pore solution is higher than below -10°C.

When the temperature of saturated concrete is reduced, the water held in the capillary pores freezes and the concrete expands. When thawing is followed by subsequent re-freezing the concrete expands further. This has a cumulative effect and is mainly in the hardened cement paste. The air filled voids in concrete due to inadequate compaction are not significantly subjected to the frost action. (Pfeifer et al 1992).

Freezing may be a slow process because of the slow rate of heat transfer through concrete and salt concentration in pore water which reduces freezing point. Also freezing starts in larger pores and slowly moves to the smaller ones. (Neville 1996)

With an increasing number of freezing cycle, the water moves to locations such as fine cracks where it can freeze. For damaged concrete, these cracks are then enlarged due to the developing pressure from ice formation and on subsequent thawing they remain filled with water. This process repeats itself during every freeze- thaw cycle.

When a closed container is filled more than 91.7% of its volume with water and is allowed to freeze, the container gets filled with ice. However, this may not be the case with concrete where the critical saturation depends on the homogeneity, size of the specimen and the rate of freezing. The main factors governing freeze-thaw resistance are the degree of saturation and the pore system of concrete. It was found that below a critical degree of saturation concrete is highly resistant to frost and dry concrete is never affected by freezing and thawing. (Powers 1955). However, not all the pore space in a water cured specimen is filled with water and that is the reason the specimen does not fail in the first freezing cycle. (Ho and Lewis 1988) Also, on rewetting concrete after it has been dried partially, it will not absorb the same amount of water it lost. (Schiessl and Raupach 1989) Hence, it is desirable to dry concrete before exposing it to freezing conditions.

Thus, it is necessary to ensure that concrete exposed to frost has low w/c ratio so that the volume of capillary pores is minimum. Also, sufficient hydration must be ensured before freezing. This makes the concrete less permeable and will not absorb much moisture. It is found that the freezing temperature decreases with the age due to increase in the salt concentration in the remaining water. (Verbeck and Kleiger 1958). And, the addition of air entraining admixture will also improve the resistance of concrete subjected to freeze-thaw cycles.

2.1 Air Entrainment and Freeze-thaw Durability

The main damage in concrete subjected to freeze-thaw cycles is caused mainly due to the expansion of water in capillary pores and this causes the ice to move through the pore system. If adjacent air voids are present, the water can escape into the voids thereby reducing the damage. This is the principle of air entrainment.

But the capillary pore volume must be minimized otherwise the volume of freezable water may exceed that which can be accommodated by the entrained air. The capillary pore volume can be reduced by ensuring a low w/c ratio. According to ACI 201.2R, concrete should not have w/c ratio more than 0.5 to be resistant to freezing and thawing and for thin sections this is reduced to 0.45.

The entrained air voids have a diameter of about 50 μm and the entrapped air voids are much larger. The air entraining admixture forms an air void matrix such that no channels for the flow of water are formed and permeability is not increased. The air entraining agents or surfactants are long chain molecules that orient themselves to reduce the surface tension of water leaving one end directed towards air in the mixture (hydrophobic) and a negatively charged hydrophilic pole. The surfactants are anionic and leave a negative charge around the voids. The negative charge help the bubbles stay anchored in the paste. (Neville 1996)

2.2 Experimental Evaluation of Freeze-Thaw Durability

2.2.1 Standard Evaluation Methods

The standard method used in the industry to evaluate the freeze-thaw resistance of concrete is according to ASTM C 666 / AASHTO T161. Two procedures were described,

- Procedure A - Rapid Freezing and Thawing in Water

- Procedure B - Rapid Freezing in Air and Thawing in Water.

These procedures are used to evaluate the variations in the properties of concrete subjected to rapid freeze – thaw cycles.

The apparatus consists of a suitable chamber/chambers where the specimens will be subjected to the specified freezing-and-thawing cycle, along with the required refrigerating and heating equipment and is also provided with controls to produce automatically and continuously, reproduce cycles within the specified temperature requirements. It is also provided with Temperature-Measuring Equipment i.e., resistance thermometers, thermometers or thermocouples to measure the temperature at various points within the chamber and at the centers of the controlled specimens. The dynamic modulus and change in length are the parameters that are evaluated using this standard, which gives us information about the loss in resistance.

2.2.2 Non-Destructive Evaluation Methods

Other means such as ultrasonic testing have also been successfully used to assess freeze-thaw damage. Molero et al. 2012, carried out an experimental study to verify the use of ultrasonic imaging, changes in through-wave velocity and attenuation measurements, as an evaluation tool for concrete subjected to freeze-thaw cycles.

2.2.3 Destructive Evaluation Methods

Shang et al. 2009, investigated the behavior of air entrained concrete subjected to freeze-thaw cycles. After 24 hours, the specimens were removed from molds and then cured for 23 days at 20 ± 3°C and 95% RH. Few specimens were immersed in water for 4 days before freeze-thaw exposure. In a single cycle that lasts about 2.5 – 3.0 hours, the specimens cooled from 6°C to −15°C and then warmed to 6°C again. The concrete specimens were subjected to 0, 100, 200, 300 and 400 freeze-thaw cycles. The dynamic modulus of elasticity, weight loss, compressive

strength, tensile strength and cleavage strength were measured. It was found that the dynamic modulus of elasticity and the strength decreased with increasing number of cycles as shown in Figure 1. As previously stated, the study concluded that crack formation mainly due to the expansion and stresses created by freezing of water and thermal stress developed during the cyclic action was responsible for the loss in mechanical properties.

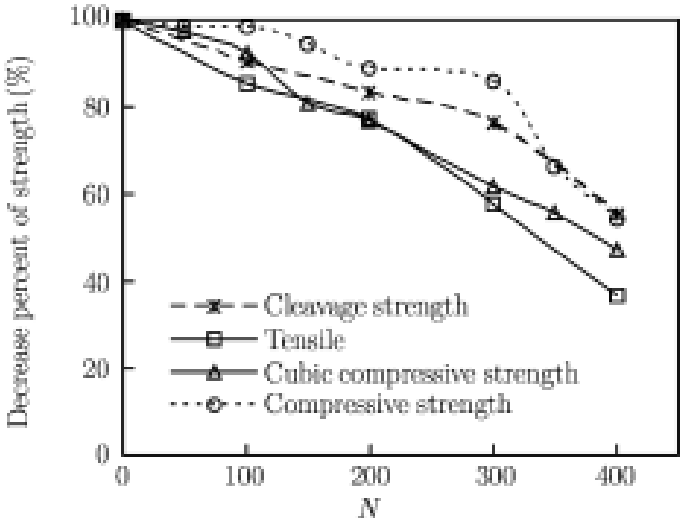

Figure 1: Decreasing percent of strength with increasing cycles of freeze-thaw

(Source: Shang et al. 2009)

Shang et al. (2009) demonstrated that as the freeze-thaw cycles were repeated, the dynamic modulus of elasticity and strength decreased. The cracks in concrete subjected to freeze-thaw are mainly due to freezing of water, its expansion and the stresses created and the thermal stress developed during the cyclic action.

2.2.4 Acoustic Emission Methods

Weiss et al., 2013, utilized acoustic emission techniques to assess freeze-thaw behavior of mortar specimens exposed to different proportions of NaCl solutions. A comparative calorimeter was

used to perform cyclic freeze- thaw testing. Ice formation and cracking were detected by monitoring heat flow and acoustic emission activity during freeze-thaw cycling.

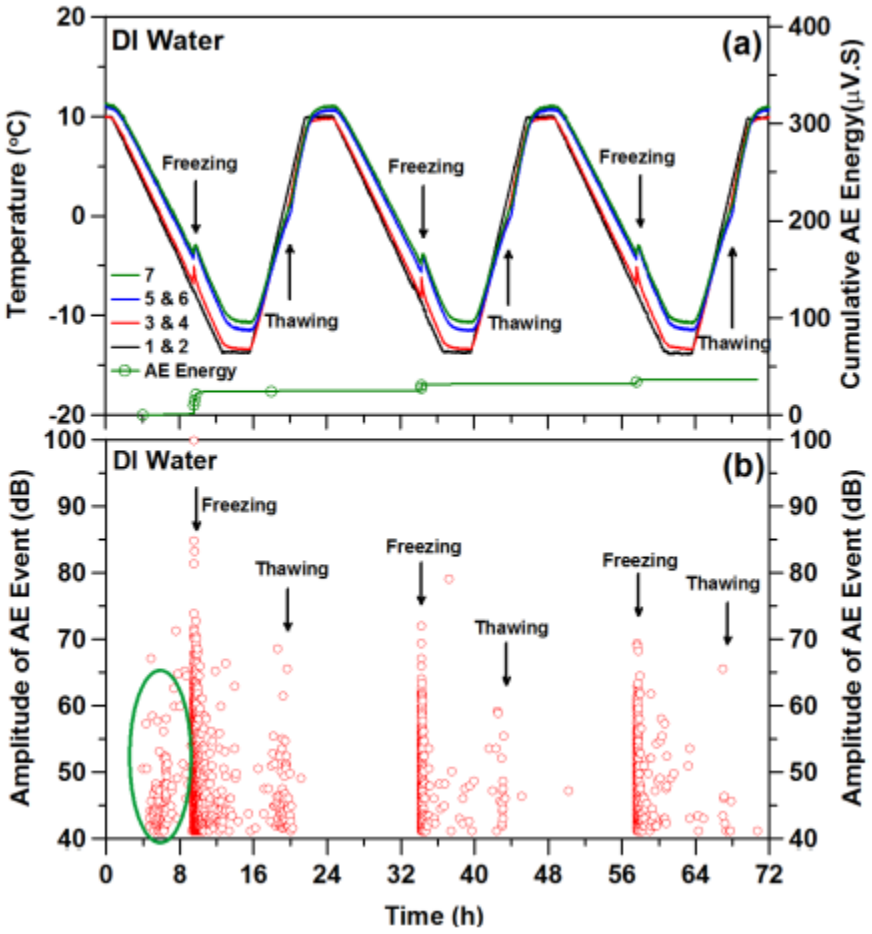

Figure 2: AE vs Temperature Cycles

(Source: Weiss et al. 2014)

Freeze-thaw cycles were carried out on mortar samples saturated with different concentrations of NaCl solutions. Active and passive acoustic emission tests were performed. Passive AE events were observed for the NaCl solutions in mortar at freezing temperature. The freeze-thaw damage was evaluated by calculating AE energy and damage parameters. It was observed that specimens immersed in de-ionized water of 0.0%, 0.7%, 3.0% and 10.0% NaCl solution, the temperature for freezing decreased with an increase in NaCl concentration due to dissolved ions and pore

confinement. AE events were recorded during the freezing phase. There was an increase in cumulative acoustic energy and damage parameter as the number of freeze-thaw cycles increased. The damage increased with an increase in NaCl concentration. The AE energy and damage parameter of specimens saturated with 23.3% NaCl solution are observed to be close to dry samples i.e., it did not show much freeze-thaw damage. (Weiss et al, 2014).

In Figure 2, it is shown that the acoustic events begin to occur as temperature of the specimen decreases. A cluster of AE events was observed in the first cycle of freeze thaw due to microcracking caused by thermal expansion coefficient mismatch between the aggregates and cement. This phenomenon was not observed from the second cycle as there was no coefficient mismatch. Endothermic peak was observed during the heating process and this is due to the thawing of ice in contact with the pore solution. It was noticed during microscopic investigations of the damaged specimens that the internal cracking was well distributed throughout the specimen and frequently occurred at aggregate – paste interface and around air voids. (Weiss et al.2013)

2.3 Overview of Acoustic emission Monitoring

Structural monitoring and testing using acoustic emission techniques have been used for a while now, because of their sensitivity to damages occurring in a structure. This was explained from a study performed on reinforced concrete beams of a bridge in which AE activity was recorded based on Kaiser's effect for incremental loading versus unloading cycles. By routinely monitoring the change in energy and amplitude, the deterioration process and mechanism can be evaluated. Failure may be shown by an increase in hits, counts and events. (Ohtsu et al. 2002; Yuyama et al. 1999). The behavior of reinforced concrete slabs under fatigue loading can be monitored using similar techniques (Yuyama et al. 2001). Acoustic emission is a versatile technique which may be used to assess various degradation behaviors related to freeze-thaw durability

For Example, Chang et al (2015), investigated AE activity of carbon fiber-reinforced polymer (CFRP) strengthened reinforced concrete beams subjected to environmental conditions where the interface between concrete and CFRP gradually deteriorates over time. Herein, acoustic emission monitoring was used to evaluate the flexural strength performance of CFRP-strengthened reinforced concrete beams subjected to freeze-thaw cycles as the condition is not visible from outside. It was found that AE parameters can be used to evaluate the performance of strengthened reinforced concrete beams that have been exposed to freeze–thaw cycles. After 400 cycles, low b-values were obtained regardless of the type of CFRP used. To better understand the viability of these methods, the following section will summarize its theoretical principles.

2.3.1 Stress-Wave Propagation Theory

Stress wave propagation theory has been employed in many non-destructive testing (NDT) of concrete. Many characteristics of concrete may be assessed using ultrasonic and acoustic emission signals. (Malhotra and Carino 1991; Uomoto 2000). The propagation of stress waves in a material may be categorized into three different modes as shown in Figure 3: "(1) compressional waves (also called longitudinal or P-waves), (2) shear waves (also called transverse or S-waves), (3) and surface waves (also called Rayleigh waves)" (Naik et al. 2004). Each of these waves travel in their own distinctive velocity (Eq. 1 to 3). Empirical correlations between wave velocity and mechanical properties based stress-strain behavior have been developed for concrete. (Eq. 4).

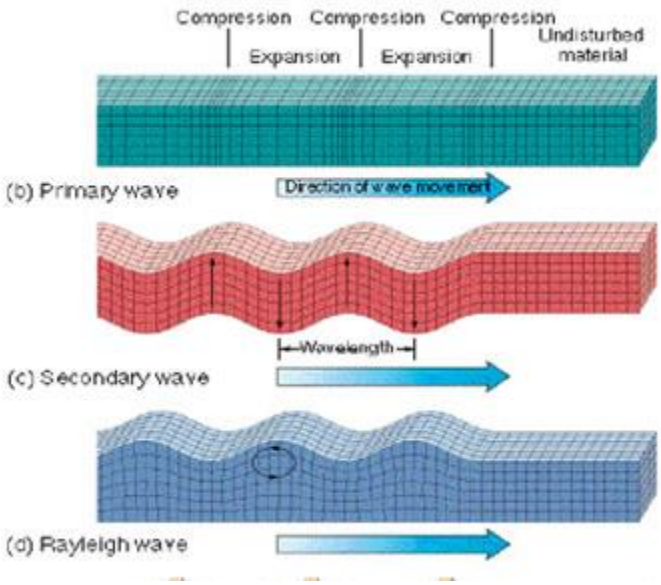

Figure 3: Particle motion related to wave mode propagation types through a solid medium:

a) Compressional wave, b) shear wave and c) Rayleigh wave.

(Source: http://electronicfieldtrip.org/volcanoes/teachers/classroom_causes.html)

The velocity of a transient wave is always constant; its value will not change with the distance travelled. Thus, the velocity of a transient wave is dependent on the elastic modulus and density of the material and is independent of the distance travelled. This can be shown by the wave velocity equation. (Eq. 5). Cut concrete is a heterogeneous material. Therefore, when a transient wave propagates through concrete it will encounter changes in boundaries which implies changes in density of the medium. This will cause changes to the velocity of the transient wave. When a transient wave strikes a boundary, a portion of the incident wave will be reflected back into the medium at the same velocity due to the change in density at the boundary. The other portion of the transient wave will travel through the second medium at a different velocity. The degree of reflection of the reflected and refracted wave is dependent on the acoustical impedance of the medium. (Eq. 6 and 7). When the transient wave propagates from one medium to the other, the frequency of the incident wave does not change but the characteristics of the wave such as the

energy and amplitude will be reduced. “This loss in energy and amplitude is referred as wave attenuation. (Carino 1997) (Mistras Group Inc. 2011).”

$$Cp = \sqrt{\frac{E(1-v)}{\rho(1+v)(1-2v)}} \quad \text{…Eq.1}$$

Where,

Cp: P-wave velocity

V: Poisson’s ratio

E: Modulus of Elasticity

ρ: Density

$$Cs = \sqrt{\frac{G}{\rho}} = \sqrt{\frac{E}{\rho 2(1+v)}} \quad \text{…Eq.2}$$

Where,

Cs: S-wave velocity

G: Shear modulus of elasticity

$$Cr = Cs\frac{0.87+1.12v}{1+v} \quad \text{Eq.3}$$

Where,

Cr: R-wave velocity

$$Ec = Wc1.5 \text{ x } 33f'c1/2 \quad \text{Eq.4}$$

Where,

Ec: Estimated modulus of elasticity of concrete

f’c: 28 day Compressive strength (psi)

Wc : Unit weight of concrete (lb/ft3)

$$C = f \text{ x } \lambda \quad \text{Eq.5}$$

Where,

f: Wave frequency

λ: Wavelength

$$Z = C \times \rho \quad \text{…Eq.6}$$

Where,

Z: Impedance of the medium

C: wave velocity

ρ: Density

$$R = \frac{Z2-Z1}{Z2+Z1} \quad \text{…Eq.7}$$

R: Reflection coefficient

Z1: Acoustic impedance of medium 1

Z2: Acoustic impedance of medium 2

The energy of the wave will reduce as it propagates from one medium to the other due to energy absorption and particle friction. The amplitude of the wave will also reduce as it propagates from one medium to the other until the energy is dissipated. But the speed and frequency of the wave will be same as the wave propagates. (Mistras Group Inc. 2011).

"Lastly, if a signal is generated through a mechanical impact or a release of elastic energy by the material itself, the incident signal containing a wide frequency spectrum will decompose into its component frequencies as it travels through the medium. This dispersive process also causes amplitude attenuation as the incident energy is dispersed into the multiple signals traveling at different wavelengths. (Mistras Group Inc. 2011) (Carino 1997)". Therefore, wave propagation theory may be employed to assess the characteristics of materials. It can be used to evaluate mechanical properties of concrete in a non-destructive manner.

2.3.2 Acoustic Emission Technique

Acoustic emission is the phenomena by which transient elastic waves are generated due to the release of energy from localized sources within the material. This release in energy is generally the causal effect of an external stimulus which may be mechanical, physical or chemical in

nature. During an ongoing event, acoustic emissions are produced and these elastic waves move towards the surface of a material, where they can be detected by sensors. The velocity of a stress or mechanical wave through any material is directly related to the elastic constant and density of the material. The sensors convert the mechanical waves into electrical signals which can be analyzed to qualify and to locate the possible source of the event. (Carpinteri et al. 2007).

Figure 4, below represents a typical acoustic emission system setup. The transducers are usually very sensitive piezoelectric sensors. The AE sensors are sensitive to a particular frequency and are usually resonance sensors. A preamplifier is connected to the AE sensor as the AE signals are very weak and in order to minimize the noise interference and prevent the signal loss. The transducer and the preamplifier are at times built as a unit. The signals then pass through a noise reduction filter to eliminate the noise. The main amplifier is used to amplify the signals before being sent to the signal conditioner. The AE features are then stored in a computer for further analysis. Figure 5, illustrates a typical waveforms recorded along with noted AE parameters of interest for analysis (Huang et al. 1998), each AE parameter is subsequently defined.

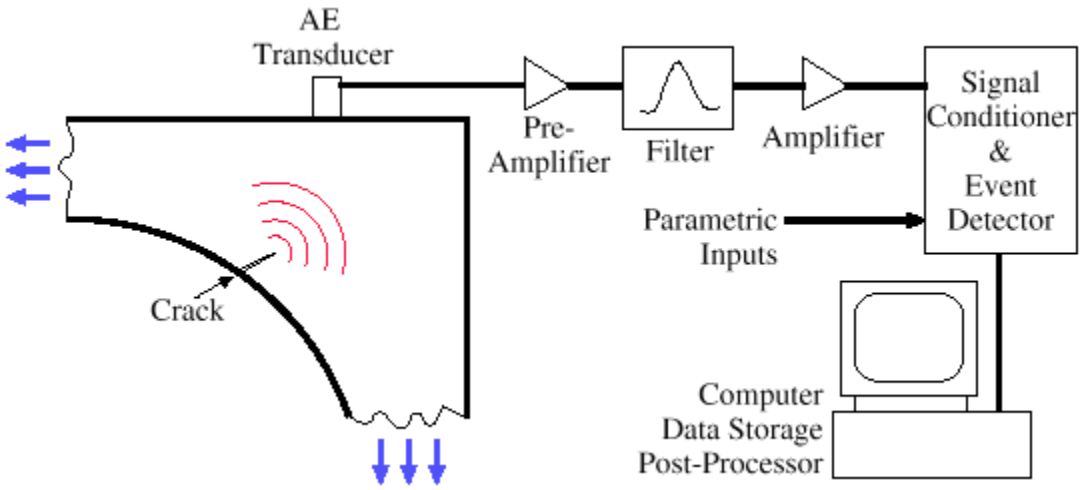

Figure 4: Schematic representation of acoustic emission testing.

(Source: Huang et al. 1998)

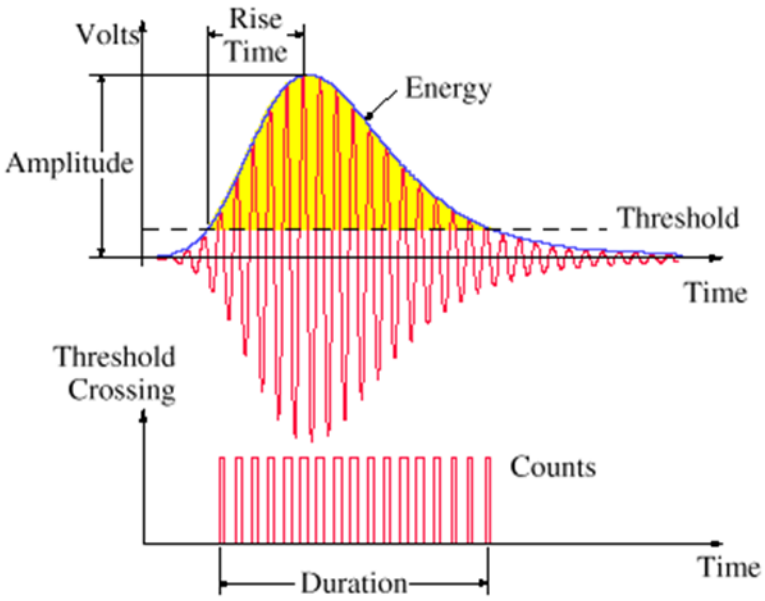

Figure 5: Waveform Parameters of AE Signal

(Source: Huang et al. 1998)

- **Threshold:** Minimum measured voltage in a waveform and is measured in decibels (dB) to trigger measurement circuitry for recording waveform.
- **Amplitude:** Greatest measured voltage in a waveform and is measured in decibels (dB).
- **Rise Time:** The time interval between the first threshold crossing and the signal peak.
- **Energy:** Measured area under the rectified signal envelope. Indication of source event's magnitude.
- **Counts:** The number of times the AE signal crosses the detection threshold.
- **Duration:** Time difference between the first and last threshold crossing.
- **Hits:** The detection and measurement of an AE signal on a channel.

Amplitude is an important parameter in AE monitoring and often used to characterize an AE event related to micro cracking and fracture processes. (Aggelis et al.2013) The loss of signal amplitude with an increasing distance from the source is defined as the attenuation. The sensor

spacing and position is governed by this which affects signal detectability. Inefficient monitoring may result due to inadequate sensor spacing if source signals are lower than the amplitude threshold to filter noise. The rate of attenuation or attenuation versus distance relationships can be found before testing by performing certain experiments to determine the material properties. (Mistras Group Inc. 2011). Therefore, to make the most use of acoustic emission technique, we must properly understand the possible limitations and the properties of the material.

CHAPTER 3

EXPERIMENTAL METHODOLOGY

Structural health monitoring techniques are often used to assess the performance of structures to evaluate their serviceability thus ensuring commuter safety. In this study, concrete samples were fabricated and subjected to freeze-thaw cycles. The material's response was monitored using acoustic emission techniques. This study evaluates the potential of acoustic emission methods to monitor the deterioration of concrete subjected to extreme temperatures. The experimental methodology established is presented in the following sections.

3.1 Sample Preparation

The methods by which the specimens were prepared and conditioned prior to freeze-thaw exposure is described in the following section. The materials used in the making of concrete, method of casting the concrete specimens, quality control and the exposure conditions they were subjected to are described below.

3.1.1 Materials

Standard materials were used in the preparation of the concrete mixtures to cast two types of samples (cylinders and prisms). The concrete mixtures were made with a natural fine aggregate (Dover sand) and a dolomitic limestone coarse aggregate (Richard Spur), which met the ASTM C 33 standard for concrete coarse and sand composition and gradation. The cement used is a Type I Portland cement (ASTM C150 / C150M), Red rock fly ash of class C (ASTM C 618) was used in

partial replacement to achieve desired water-to-cementitious material. Tap water from the city supply of Stillwater, Oklahoma, was used. The water source was considered to be potable and hence, no quality control testing was performed on the mixing water. A liquid air-entraining agent, Daravair 1000, was also used in order to increase the yield control and provide adequate void matrix to increase freeze-thaw resistance of the mixture.

The mixture was designed using ASTM C 685/C 685M – 01. The w/c ratio for the present study was 0.45 and the mixture design was similar to meet the requirements of Oklahoma Department of Transportation. Air entraining admixture was added to the mixture to obtain a percent air content between 5% and 8%. The mixture design is detailed in Table 1.Only one mixture was designed and used since the study concentrated on evaluating the performance of concrete subjected to freeze-thaw cycles using acoustic emission techniques.

Table 1: Mixture Design Sheet

Material	Description	Quantity (Kg/m^3)
Water	Potable, city of Stillwater, Oklahoma	161.151
Cement	Type - 1	289.636
Coarse aggregate	5-14 mm	1087.834
Fine aggregate	0-5 mm	708.052
Fly ash	Red rock	72.389
Air Entrainer	Daravair 1000	12 ml

3.1.2 Casting

The cylinder and prism specimens were cast within the controlled environment of the civil engineering laboratory at Oklahoma State University. The specimens were prepared, mixed and cast according to the procedures described in ASTM C 172 and ASTM C 192 standards. Standard procedures were followed to maintain quality control of the concrete specimens. The unit weight,

air contents and slumps were measured for each of the concrete batch. (C 138/C 138M, ASTM C 143 and ASTM C 231). The design values were 6% for air content and 203 mm for slump. Measured values of unit weight, air content and slump varied less than ±10% between batches and are shown in Table 2.

Table 2: Fresh concrete properties

Batch	Mass of measure (Kg)	Mass of concrete (Kg)	Unit Weight (Kg/m^3)	Slump (mm)	Air content (%)
1	4.15854	20.01354	2239.656	200	9
2	4.15854	20.48466	2306.206	190	5.6
3	4.15854	20.68398	2334.362	200	5
4	4.15854	20.26722	2275.491	210	7.4

1. Slump Test – a method used to find the consistency of fresh concrete and was carried out in accordance with ASTM C143 / C143M.
2. Unit weight of concrete – The unit weight of concrete was calculated according to ASTM C138 / C138M.
3. Air content test – Air meter was used to calculate the percentage of air in fresh concrete according to ASTM C231 / C231M.

Four batches of concrete were made with each batch measuring 0.055 m3 and approximately 50 cylinders and 20 prism specimens were made from the 4 batches. The dimensions of the specimens are as follows:

- 20 rectangular prisms – 75 mm x 75 mm x 410 mm
- 50 cylinders - ø100 mm x 200 mm

The cylindrical molds measuring ø100 mm x 200 mm met the requirements specified in ASTM C 470. The prism molds measuring 75 mm x 75 mm x 410 mm met the requirements specified in ASTM C 78. The prism and cylinder specimens were prepared in two equal layers with external vibration to consolidate the fresh concrete into the molds.

3.1.3 Sample Curing and Conditioning

A moist curing environment was prepared and the samples were placed in it after the initial set had occurred. The samples were covered with wet burlap which was loosely sealed under a plastic tarp. The samples were demolded after a period of 24 hours and, all the specimens were cured in a moist curing room at 20±3˚C and 95% relative humidity for 28 days. After curing, they were taken out of the moist curing room and allowed to dry for 48 hours in ambient laboratory conditions. The specimens were then conditioned at 23˚C and 60% relative humidity in an environmental chamber for seven days.

3.2 Freeze-Thaw Exposure Regimen

The following section describes how the temperature profile was analyzed. This includes a description of exposure regimen and the details of the freeze- thaw chamber used.

3.2.1 Temperature Profile

Historical temperature data was analyzed for Oklahoma City. Daily extremes were analyzed for Oklahoma City for a period of 11 years, from January 2004 to December 2014. The temperature data was obtained from http://www.usclimatedata.com/. The daily maximum and minimum temperatures was plotted for the 11 years. Temperatures were recorded to the nearest 0.1°C. Variance of the daily maxima and minima were calculated for every month and the critical temperatures or the peak low temperatures were found to be during the months of December, January and February. The peak, average and the standard deviation of the daily minimum temperatures were computed for the three months. The difference between the average and the standard deviation was computed for each of the three months and it was found that the daily minimum recorded was most of the times greater than this value. This value was computed for

each year under consideration and the average value for the 11 year period is used as the test temperature. Values are presented in Table 3.

Table 3: Statistical analysis of Recorded Daily Low Temperature for the months of December, January and February (Coolest months of the year)

Average of Recorded Daily Low Temperature (˚C)											
	2004	2005	2006	2007	2008	2009	2010	2011	2012	2013	2014
Jan	-1.48	-1.27	0.95	-2.25	-2.28	-4.30	-2.87	-5.20	-0.53	-1.11	-3.88
Feb	-1.76	2.85	-1.48	-0.57	-1.43	1.86	-1.59	-1.71	1.23	-0.27	-2.52
Dec	-0.27	-2.78	0.39	-1.62	-2.70	-4.07	-1.31	-0.48	-0.22	-3.37	2.09
Standard Deviation(˚C)											
	2004	2005	2006	2007	2008	2009	2010	2011	2012	2013	2014
Jan	6.90	5.45	4.09	4.49	6.18	3.91	6.14	4.42	4.23	5.51	5.32
Feb	4.37	3.98	5.35	6.32	3.70	5.51	2.91	9.85	4.77	3.41	5.44
Dec	5.43	4.98	5.57	3.75	5.90	4.02	4.35	3.97	6.21	5.66	5.27
Average Minus One Standard Deviation (˚C)											
	2004	2005	2006	2007	2008	2009	2010	2011	2012	2013	2014
Jan	-8.38	-6.72	-3.14	-6.74	-8.46	-8.21	-9.01	-9.62	-4.76	-6.62	-9.20
Feb	-6.13	-1.13	-6.83	-6.88	-5.13	-3.66	-4.49	-11.56	-3.53	-3.68	-7.96
Dec	-5.70	-7.76	-5.18	-5.38	-8.59	-8.09	-5.65	-4.46	-6.43	-9.03	-3.18
Average	-6.40										

3.1.1 Exposure Regimen

The exposure conditions for the concrete specimens were simulated using the Endurance standard temperature & humidity test chamber which is manufactured by ENVIROTRONICS. (Figure. 6) The chamber is capable of simulating temperatures in the range of -40 and +180 ˚C. 18 cylinders

were arranged on three shelves and 6 prisms were placed at the bottom of the chamber. In the chamber, the samples were subjected to freeze-thaw cycles. Each freeze-thaw cycle lasted for a period of 30 hours as shown in Figure7. Prior to exposure regimen, the samples were sealed using a plastic wrap to maintain the 60% relative humidity previously achieved during the sample conditioning period. However, the monitored samples were first prepared has described in the following section.

Figure 6: Samples placed in environmental chamber for exposure regimen

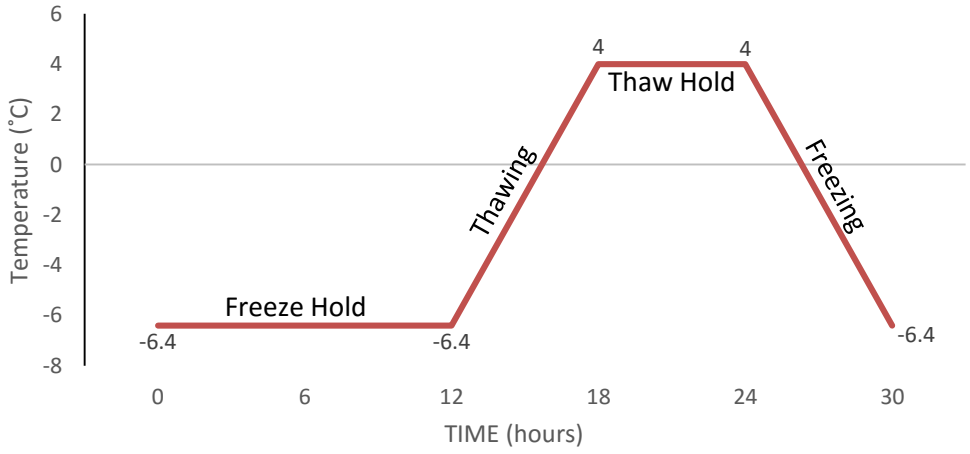

Figure 7: Single freeze – thaw cycle

3.3 Acoustic Emission Monitoring Techniques

Acoustic emission monitoring techniques were used to quantify the damage caused in a specimen subjected to freeze-thaw cycles. The techniques used for monitoring may be classified as active or passive acoustic emission. In the active acoustic emission technique, the wave speed is measured by the use of a pulsed wave and in the passive acoustic emission technique, the waves generated due to freeze-thaw activity are recorded. In the present study, to measure the damage due to freeze-thaw cycles, the passive acoustic emission technique was used. Two sensors were attached to the specimens using an epoxy glue for the acoustic emission measurements as shown in Figure 8.

Figure 8: Sensor glued to the specimen

AE is proven to be a useful tool to monitor ongoing physical and chemical changes within a specimen. In this case, AE monitoring was used to detect events within the concrete samples. These events caused by external loading are assumed to be linked to the initiation and propagation of micro cracks. The Express -8 AE system manufactured by Mistras was used. Two cylinders and two prisms with sensors placed at the ends were monitored using the AE acquisition system. A series of parameters related to the hardware and software were entered in

AEWIN. These parameters were chosen according to common practice in acoustic emission monitoring of concrete structures. The wave speed of the concrete sample must be first determined to localize the AE events. The averages of the longitudinal 54 kHz and 150 kHz from the UPV testing were compared to obtain the wave speed of the sample.

3.3.1 AE Hardware

The selection of an AE sensor depends on the specific application. In our research, a wide band sensor as shown in Figure 9 was used. A small diameter AE sensor with high frequency bandwidth was glued to the specimen using epoxy. Two sensors were fixed at either ends of the specimen.

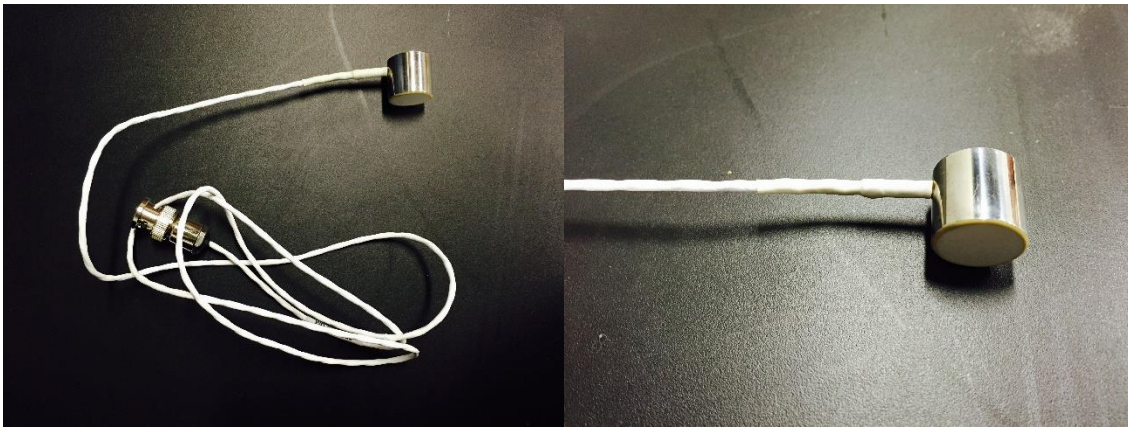

Figure 9: Wide band sensors

The AE signal from the sensor must be amplified before it is transmitted to the measurement circuitry and for this purpose the 2/4/6 preamplifier from Mistras group was used. The preamplifier is provided with three selectable gain ranges where 2/4/6 refers to 20 dB, 40dB and 60 dB gain ranges as shown in Figure 10. These preamplifiers can be operated as a single-ended or for differential inputs. For our study the 40 dB gain differential selection was used.

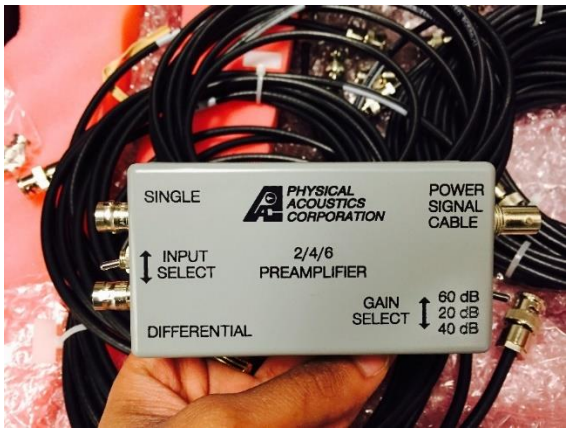

Figure 10: 2/4/6 Amplifier

3.3.2 AE Software

The AEwin software from Mistras group was used for real time recording of acoustic emissions. The software is capable of recording several acoustic emission parameters and displays detailed information on the selected data and also plots them on graphs. Auto Sensor Test can also be performed using the software.

3.3.3 Background Noise

Various sources such as frictional, impact loading, liquid flow, and electromagnetic noise could be attributed to AE signals. The operation of the freeze – thaw machine by itself will produce electromagnetic noise along with acoustic noise, which generates undesired acoustic emission signals during the test for crack detection. Therefore, noise control in AE monitoring is significant as this will influence the reliability and accuracy of the results.

There are a lot of techniques developed to filter the noise in the testing environment (Pollock. 1989) and one of the most important step will be the selection of the frequency range. Electrical noise can also be removed by high-end AE sensors and preamplifiers. Band-pass filters will be useful to eliminate the audible noise (lower frequency than the testing configurations). Advanced

techniques such as the floating threshold and front-end filtering can also be incorporated. The AE software and hardware also provides with different options to control noise. Concerning the issues above, 45 dB was selected as the threshold for the present research.

Thereafter, during monitoring, several AE signals stood out from the rest of the data set; the energy and amplitude were very high in comparison to other AE activity. Moreover, the noise was recorded from all sensors. This is a sign that the event was not related to sample activity; therefore, not considered in the analysis. It may potentially have been from some external noise due to disturbance in the laboratory environment.

The greatest measured voltage in a waveform is referred to as amplitude which is measured in decibels (dB). It is one of the most significant parameters in acoustic emission assessment as it provides information on the detectability of a signal. A minimum threshold of 45 dB was used to cancel out amplitudes due to external noise. The reliability of results was found to increase with signals of higher amplitude. Energy is the measured area under the rectified signal envelope. It is an indication of source event's magnitude. The source signal will produce larger amplitude and energy when more material is undergoing strain. Thus, high energy and high amplitude events was considered for the AE monitoring technique.

CHAPTER 4

RESULTS AND DISCUSSION

As described in section 3.3, AE data was recorded using AEWin software by Mistras for fifteen temperature cycles. For this analysis, the time versus AE data was overlapped with the time versus temperature data from the ENDURANCE freeze-thaw chamber. The recorded AE activity according to temperature was then plotted for all 15 cycles (Appendix A). Based on the latter, the following sections present a detailed analysis of the measured amplitude and energy levels during each stage of the temperature cycle: freezing phase, freeze-holding phase, thawing phase, thaw-holding phase.

The number of hits, amplitude and energy recorded in each phase was tabulated. The amplitude was categorized into different ranges (i.e. less than 50, 50-60, 60-70 and 70-80) with 45 and 80 being the minimum amplitude recorded. The energy recorded was also categorized into ranges of 0 – 200, 200-400 up to 1000 and 1000 – 2000. The established categories enable a better analysis of the source events. The larger the number of counts or hits and the larger the amplitude and energy the source signal will generate, the more material may be involved in the process. It is an indication of the degree in emissivity which may be related to changes in material properties and failure mechanisms Therefore, the amount of events of high amplitude and energy was considered in the analysis. It is an indication of the degree in emissivity which may be related to changes in material properties and failure mechanisms of a sample under stress. (Pollock 1989)

4.1 Damage Analysis During Freezing Phase

4.1.1 Amplitude and Number of Hits

The number of hits per amplitude range for each specimen per cycle is shown through Tables 4 to 7. First, it needs to be addressed that the results from channel 1 are not reliable as the amplifier connected to this channel may not have been functioning properly. The peak amplitude was observed to be 60 dB for channel 5 (prism specimen 3) for cycle 7 and also for channel 7 (prism specimen 4), cycle 2. When the temperature of concrete decreases the water in the capillary pores freeze and concrete expands which causes cracking. As mentioned earlier in section 2.1, freezing starts in capillary pores this causes the ice to move through the pore system. This may be the reason for more hits at the earlier cycles. More number of hits are in the range of <50 dB, this may imply that there was microcracking with small amplitudes.

Table 4: Number of AE hits per amplitude range during freezing phase for cylindrical specimen 1, channel 1 and 2.

Cycle	**Number of Hits per Amplitude Range (dB)**									
	< 50		**50-59**		**60-69**		**70-79**		**80 <**	
	Channel									
	1	**2**	**1**	**2**	**1**	**2**	**1**	**2**	**1**	**2**
1	-	-	-	-	-	-	-	-	-	-
2	-	3	-	-	-	-	-	-	-	-
3	-	-	-	-	-	-	-	-	-	-
4	-	1	-	-	-	-	-	-	-	-
5	-	-	-	-	-	-	-	-	-	-
6	1	-	-	-	-	-	-	-	-	-
7	-	-	-	-	-	-	-	-	-	-
8	-	-	-	-	-	-	-	-	-	-
9	-	-	-	-	-	-	-	-	-	-
10	-	1	-	-	-	-	-	-	-	-
11	-	-	-	-	-	-	-	-	-	-
12	-	-	-	-	-	-	-	-	-	-
13	-	1	-	1	-	-	-	-	-	-
14	-	-	-	-	-	-	-	-	-	-
15	-	-	-	-	-	-	-	-	-	-
Total	1	6	0	1	0	0	0	0	0	0

Table 5: Number of AE hits per amplitude range during freezing phase for cylindrical specimen 2, channel 3 and 4.

Cycle	Number of Hits per Amplitude Range (dB)									
	< 50		50-59		60-69		70-79		80 <	
	Channel									
	3	4	3	4	3	4	3	4	3	4
1	-	-	-	-	-	-	-	-	-	-
2	1	-	-	1	-	-	-	-	-	-
3	-	-	-	-	-	-	-	-	-	-
4	-	1	-	-	-	-	-	-	-	-
5	-	-	-	-	-	-	-	-	-	-
6	-	-	-	1	-	-	-	-	-	-
7	1	3	2	-	-	-	-	-	-	-
8	-	-	-	-	-	-	-	-	-	-
9	-	-	-	-	-	-	-	-	-	-
10	-	-	-	-	-	-	-	-	-	-
11	-	-	-	-	-	-	-	-	-	-
12	-	-	-	-	-	-	-	-	-	-
13	-	-	-	-	-	-	-	-	-	-
14	-	-	-	-	-	-	-	-	-	-
15	-	-	-	-	-	-	-	-	-	-
Total	2	4	2	2	0	0	0	0	0	0

Table 6: Number of AE hits per amplitude range during freezing phase for prism specimen 3, channel 5 and 6.

Cycle	Number of Hits per Amplitude Range (dB)									
	< 50		50-59		60-69		70-79		80 <	
	Channel									
	5	6	5	6	5	6	5	6	5	6
1	-	1	-	1	-	-	-	-	-	-
2	1	1	3	2	-	-	-	-	-	-
3	-	-	-	-	-	-	-	-	-	-
4	-	-	-	-	-	-	-	-	-	-
5	-	-	-	-	-	-	-	-	-	-
6	-	-	-	1	-	-	-	-	-	-
7	-	-	-	1	1	-	-	-	-	-
8	-	-	-	-	-	-	-	-	-	-
9	-	-	-	-	-	-	-	-	-	-
10	-	-	-	-	-	-	-	-	-	-
11	-	-	-	-	-	-	-	-	-	-
12	1	-	-	-	-	-	-	-	-	-
13	-	-	-	-	-	-	-	-	-	-
14	1	-	-	-	-	-	-	-	-	-
15	2	-	-	-	-	-	-	-	-	-
Total	5	2	3	5	1	0	0	0	0	0

Table 7: Number of AE hits per amplitude range during freezing phase for prism specimen 4, channel 7 and 8.

Cycle	Number of Hits per Amplitude Range (dB)									
	< 50		50-59		60-69		70-79		80 <	
	Channel									
	7	8	7	8	7	8	7	8	7	8
1	2	2	-	-	-	-	-	-	-	-
2	1	3	1	1	1	-	-	-	-	-
3	-	-	-	-	-	-	-	-	-	-
4	-	-	-	-	-	-	-	-	-	-
5	-	-	-	-	-	-	-	-	-	-
6	-	1	1	-	-	-	-	-	-	-
7	-	-	1	1	-	-	-	-	-	-
8	-	-	-	-	-	-	-	-	-	-
9	-	1	-	-	-	-	-	-	-	-
10	1	-	-	2	-	-	-	-	-	-
11	-	-	-	2	-	-	-	-	-	-
12	-	-	-	-	-	-	-	-	-	-
13	-	-	-	-	-	-	-	-	-	-
14	-	1	-	-	-	-	-	-	-	-
15	-	-	-	-	-	-	-	-	-	-
Total	4	8	3	6	1	0	0	0	0	0

4.1.2 Energy and Number of Hits

The number of hits per energy range for each specimen per cycle is shown through Tables 8 to 11. The peak energy was observed to be 10833 at channel 8 (prism specimen 4) for cycle 14. This high energy is accompanied with amplitude of 45 dB. Most hits are between 0-399 uJ and most of these hits have their amplitudes <50 (section 4.1.1), this shows that the event that occurred may be due to the generation of microstructural damage. Still, in comparison to Weiss et al. 2014, the number of hits recorded is very low. Here, the freezing temperature reached may not be sufficiently low and the rate at which it may not be sufficiently high to induce microcracking related to ice formation as detailed in the literature review. Moreover, the samples were conditioned at 60% relative humidity; therefore, there may not be a sufficient amount of water to cause ice formation damage.

Table 8: Number of AE hits per energy range during freezing phase for cylindrical specimen 1, channel 1 and 2.

Cycle	Number of Hits per Energy Range									
	0-399		400-799		800-1199		1200-1600		1600 <	
	Channel									
	1	2	1	2	1	2	1	2	1	2
1	-	-	-	-	-	-	-	-	-	-
2	-	3	-	-	-	-	-	-	-	-
3	-	-	-	-	-	-	-	-	-	-
4	-	1	-	-	-	-	-	-	-	-
5	-	-	-	-	-	-	-	-	-	-
6	1	-	-	-	-	-	-	-	-	-
7	-	-	-	-	-	-	-	-	-	-
8	-	-	-	-	-	-	-	-	-	-
9	-	-	-	-	-	-	-	-	-	-
10	-	1	-	-	-	-	-	-	-	-
11	-	-	-	-	-	-	-	-	-	-
12	-	-	-	-	-	-	-	-	-	-
13	-	2	-	-	-	-	-	-	-	-
14	-	-	-	-	-	-	-	-	-	-
15	-	-	-	-	-	-	-	-	-	-
Total	1	7	0	0	0	0	0	0	0	0

Table 9: Number of AE hits per energy range during freezing phase for cylindrical specimen 2, channel 3 and 4.

Cycle	Number of Hits per Energy Range									
	0-399		400-799		800-1199		1200-1600		1600 <	
	Channel									
	3	4	3	4	3	4	3	4	3	4
1	-	-	-	-	-	-	-	-	-	-
2	1	1	-	-	-	-	-	-	-	-
3	-	-	-	-	-	-	-	-	-	-
4	-	1	-	-	-	-	-	-	-	-
5	-	-	-	-	-	-	-	-	-	-
6	-	1	-	-	-	-	-	-	-	-
7	2	2	1	1	-	-	-	-	-	-
8	-	-	-	-	-	-	-	-	-	-
9	-	-	-	-	-	-	-	-	-	-
10	-	-	-	-	-	-	-	-	-	-
11	-	-	-	-	-	-	-	-	-	-
12	-	-	-	-	-	-	-	-	-	-
13	-	-	-	-	-	-	-	-	-	-
14	-	-	-	-	-	-	-	-	-	-
15	-	-	-	-	-	-	-	-	-	-
Total	3	5	1	1	0	0	0	0	0	0

Table 10: Number of AE hits per energy range during freezing phase for prism specimen 3, channel 5 and 6.

Cycle	Number of Hits per Energy Range									
	0-399		400-799		800-1199		1200-1600		1600 <	
	Channel									
	5	6	5	6	5	6	5	6	5	6
1	-	2	-	-	-	-	-	-	-	-
2	2	2	1	1	1	-	-	-	-	-
3	-	-	-	-	-	-	-	-	-	-
4	-	-	-	-	-	-	-	-	-	-
5	-	-	-	-	-	-	-	-	-	-
6	-	1	-	-	-	-	-	-	-	-
7	-	-	-	-	-	-	-	-	1	1
8	-	-	-	-	-	-	-	-	-	-
9	-	-	-	-	-	-	-	-	-	-
10	-	-	-	-	-	-	-	-	-	-
11	-	-	-	-	-	-	-	-	-	-
12	1	-	-	-	-	-	-	-	-	-
13	-	-	-	-	-	-	-	-	-	-
14	1	-	-	-	-	-	-	-	-	-
15	2	-	-	-	-	-	-	-	-	-
Total	6	5	1	1	1	0	0	0	1	1

Table 11: Number of AE hits per energy range during freezing phase for prism specimen 4, channel 7 and 8.

Cycle	Number of Hits per Energy Range									
	0-399		400-799		800-1199		1200-1600		1600 <	
	Channel									
	7	8	7	8	7	8	7	8	7	8
1	2	2	-	-	-	-	-	-	-	-
2	2	3	1	1	-	-	-	-	-	-
3	-	-	-	-	-	-	-	-	-	-
4	-	-	-	-	-	-	-	-	-	-
5	-	-	-	-	-	-	-	-	-	-
6	1	1	-	-	-	-	-	-	-	-
7	-	-	-	-	-	-	-	-	1	1
8	-	-	-	-	-	-	-	-	-	-
9	-	1	-	-	-	-	-	-	-	-
10	1	2	-	-	-	-	-	-	-	-
11	-	2	-	-	-	-	-	-	-	-
12	-	-	-	-	-	-	-	-	-	-
13	-	-	-	-	-	-	-	-	-	-
14	-	-	-	-	-	-	-	-	-	1
15	-	-	-	-	-	-	-	-	-	-
Total	6	11	1	1	0	0	0	0	1	2

4.2 Damage Analysis during Freeze-Hold Phase

4.2.1 Amplitude and number of hits

The number of hits per amplitude range for each specimen per cycle is shown through Tables 12 to 15. The peak amplitude during the freeze–hold phase was found to be 80 dB at channel 7 (prism specimen 4), cycle 8. The corresponding energy for this amplitude was 7512 uJ, which may be related to a damaging event. As the freeze-hold phase was maintained for 12 hours (double to that of other phases), more activity i.e., hits are being observed in comparison to that observed during the freezing phase (section 4.1). This emphasizes that multiple events, potentially related to ice formation, was occurring during this phase. It was also observed that there were more hits in <50 and 50-59 dB range in this phase as compared to freezing phase (section 4.1.1). Again emphasizing, the beginning of ice formation at temperatures near -6.4°C.

Table 12: Number of AE hits per amplitude range during freeze-hold phase for cylindrical specimen 1, channel 1 and 2.

Cycle	**Number of Hits per Amplitude Range (dB)**									
	< 50		**50-59**		**60-69**		**70-79**		**80 <**	
	Channel									
	1	**2**	**1**	**2**	**1**	**2**	**1**	**2**	**1**	**2**
1	-	-	-	-	-	-	-	-	-	-
2	-	-	-	-	-	-	-	-	-	-
3	-	-	-	1	-	-	-	-	-	-
4	1	1	-	-	-	-	-	-	-	-
5	-	-	1	-	-	-	-	-	-	-
6	-	-	-	1	-	-	-	-	-	-
7	-	-	-	-	-	-	-	-	-	-
8	-	1	1	1	-	-	-	-	-	-
9	1	-	-	-	-	-	-	-	-	-
10	1	-	-	-	-	-	-	-	-	-
11	-	-	-	-	-	-	-	-	-	-
12	-	-	-	1	-	-	-	-	-	-
13	-	1	-	1	-	1	-	-	-	-
14	-	1	-	-	-	-	-	-	-	-
15	-	-	-	-	-	-	-	-	-	-
Total	3	4	2	5	0	1	0	0	0	0

Table 13: Number of AE hits per amplitude range during freeze-hold phase for cylindrical specimen 2, channel 3 and 4.

Cycle	Number of Hits per Amplitude Range (dB)									
	< 50		50-59		60-69		70-79		80 <	
	Channel									
	3	4	3	4	3	4	3	4	3	4
1	2	1	-	-	-	-	-	-	-	-
2	-	-	1	-	-	-	-	-	-	-
3	-	-	-	-	-	-	-	-	-	-
4	1	-	1	-	-	-	-	-	-	-
5	-	-	-	-	-	-	-	-	-	-
6	-	-	-	1	-	-	-	-	-	-
7	-	1	-	-	-	-	-	-	-	-
8	-	-	-	-	-	-	-	-	-	-
9	3	2	1	1	-	-	-	-	-	-
10	-	-	-	1	-	-	-	-	-	-
11	-	-	-	-	-	-	-	-	-	-
12	-	-	-	-	-	-	-	-	-	-
13	1	-	-	1	-	-	-	-	-	-
14	-	-	-	-	-	-	-	-	-	-
15	-	-	-	-	-	-	-	-	-	-
Total	7	4	3	4	0	0	0	0	0	0

Table 14: Number of AE hits per amplitude range during freeze-hold phase for prism specimen 3, channel 5 and 6.

Cycle	Number of Hits per Amplitude Range (dB)									
	< 50		50-59		60-69		70-79		80 <	
	Channel									
	5	6	5	6	5	6	5	6	5	6
1	3	4	1	-	-	-	-	-	-	-
2	-	1	-	-	-	-	-	-	-	-
3	-	-	-	-	-	-	-	-	-	-
4	-	1	-	-	1	-	-	-	-	-
5	-	-	1	-	-	-	-	-	-	-
6	2	2	-	-	-	-	-	-	-	-
7	-	-	1	1	-	-	-	-	-	-
8	-	-	-	-	-	-	-	-	-	-
9	-	-	2	2	-	-	-	-	-	-
10	-	-	-	-	-	-	-	-	-	-
11	-	-	1	-	-	-	-	-	-	-
12	3	2	-	-	1	-	-	-	-	-
13	1	2	-	-	-	-	-	-	-	-
14	1	-	-	-	-	-	-	-	-	-
15	-	1	-	-	-	-	-	-	-	-
Total	10	13	6	3	2	0	0	0	0	0

Table 15: Number of AE hits per amplitude range during freeze-hold phase for prism specimen 4, channel 7 and 8.

Cycle	Number of Hits per Amplitude Range (dB)									
	< 50		50-59		60-69		70-79		80 <	
	Channel									
	7	8	7	8	7	8	7	8	7	8
1	2	-	3	1	-	-	-	-	-	-
2	-	1	-	-	-	-	-	-	-	-
3	-	1	-	-	-	-	-	-	-	-
4	-	-	-	-	-	-	-	-	-	-
5	1	-	-	2	-	-	-	-	-	-
6	1	2	-	-	-	-	-	-	-	-
7	-	-	-	1	-	-	-	-	-	-
8	-	-	-	-	-	-	-	-	1	-
9	-	1	2	2	-	-	-	-	-	-
10	-	-	-	1	1	-	-	-	-	-
11	-	-	-	-	-	-	-	-	-	-
12	1	1	2	-	-	-	-	-	-	-
13	2	-	-	-	-	-	-	-	-	-
14	-	1	1	1	-	-	-	-	-	-
15	-	-	1	1	-	-	-	-	-	-
Total	7	7	9	9	1	0	0	0	1	0

4.1.2 Energy and number of hits

The number of hits per amplitude range for each specimen per cycle is shown through Tables 16 to 19. The peak energy was observed to 7512 uJ and may due to ice formation and damage generation in the cement paste matrix. A lot of events are observed to be having energy within the range of 0-399 uJ. This shows that minor events took place during this phase. The more number of events in this phase can be attributed to the increased duration of this phase (12 hours, double than the other phases) and more pores getting frozen leading to more number of cracks and events. As mentioned in the Literature Review, Weiss et al. (2013) reported a higher number of hits in the initial freeze-thaw cycles were higher than the later cycles and this trend is not observed in this study as the freezing and thawing temperatures were not the same. In this study, the freeze – thaw temperature followed was -14 ˚C to 10˚C and the temperature monitored in the present study was -6.4˚C to 4 ˚C. The low count of hits may be because of the water not being frozen in the capillary pores at the temperature that was considered for this study.

Table 16: Number of AE hits per energy range during freeze-hold phase for cylindrical specimen 1, channel 1 and 2.

Cycle	Number of Hits per Energy Range									
	0-399		400-799		800-1199		1200-1600		1600 <	
	Channel									
	1	2	1	2	1	2	1	2	1	2
1	-	-	-	-	-	-	-	-	-	-
2	-	-	-	-	-	-	-	-	-	-
3	-	1	-	-	-	-	-	-	-	-
4	1	1	-	-	-	-	-	-	-	-
5	1	-	-	-	-	-	-	-	-	-
6	-	1	-	-	-	-	-	-	-	-
7	-	-	-	-	-	-	-	-	-	-
8	1	2	-	-	-	-	-	-	-	-
9	1	-	-	-	-	-	-	-	-	-
10	1	-	-	-	-	-	-	-	-	-
11	-	-	-	-	-	-	-	-	-	-
12	-	1	-	-	-	-	-	-	-	-
13	-	3	-	-	-	-	-	-	-	-
14	-	1	-	-	-	-	-	-	-	-
15	-	-	-	-	-	-	-	-	-	-
Total	5	10	0	0	0	0	0	0	0	0

Table 17: Number of AE hits per energy range during freeze-hold phase for cylindrical specimen 2, channel 3 and 4.

Cycle	Number of Hits per Energy Range									
	0-399		400-799		800-1199		1200-1600		1600 <	
	Channel									
	3	4	3	4	3	4	3	4	3	4
1	2	1	-	-	-	-	-	-	-	-
2	1	-	-	-	-	-	-	-	-	-
3	-	-	-	-	-	-	-	-	-	-
4	2	-	-	-	-	-	-	-	-	-
5	-	-	-	-	-	-	-	-	-	-
6	-	1	-	-	-	-	-	-	-	-
7	-	1	-	-	-	-	-	-	-	-
8	-	-	-	-	-	-	-	-	-	-
9	3	2	-	-	-	1	-	-	1	-
10	-	1	-	-	-	-	-	-	-	-
11	-	-	-	-	-	-	-	-	-	-
12	-	-	-	-	-	-	-	-	-	-
13	1	1	-	-	-	-	-	-	-	-
14	-	-	-	-	-	-	-	-	-	-
15	-	-	-	-	-	-	-	-	-	-
Total	9	7	0	0	0	1	0	0	1	0

Table 18: Number of AE hits per energy range during freeze-hold phase for prism specimen 3, channel 5 and 6.

Cycle	Number of Hits per Energy Range									
	0-399		400-799		800-1199		1200-1600		1600 <	
	Channel									
	5	6	5	6	5	6	5	6	5	6
1	3	3	1	1	-	-	-	-	-	-
2	-	1	-	-	-	-	-	-	-	-
3	-	-	-	-	-	-	-	-	-	-
4	1	1	-	-	-	-	-	-	-	-
5	1	-	-	-	-	-	-	-	-	-
6	2	2	-	-	-	-	-	-	-	-
7	1	1	-	-	-	-	-	-	-	-
8	-	-	-	-	-	-	-	-	-	-
9	-	-	1	1	1	1	-	-	-	-
10	-	-	-	-	-	-	-	-	-	-
11	1	-	-	-	-	-	-	-	-	-
12	4	2	-	-	-	-	-	-	-	-
13	1	2	-	-	-	-	-	-	-	-
14	1	-	-	-	-	-	-	-	-	-
15	-	1	-	-	-	-	-	-	-	-
Total	15	13	2	2	1	1	0	0	0	0

Table 19: Number of AE hits per energy range during freeze-hold phase for prism specimen 4, channel 7 and 8.

Cycle	Number of Hits per Energy Range									
	0-399		400-799		800-1199		1200-1600		1600 <	
	Channel									
	7	8	7	8	7	8	7	8	7	8
1	4	1	1	-	-	-	-	-	-	-
2	-	1	-	-	-	-	-	-	-	-
3	-	1	-	-	-	-	-	-	-	-
4	-	-	-	-	-	-	-	-	-	-
5	1	1	-	-	-	-	-	-	-	-
6	1	2	-	-	-	-	-	-	-	-
7	-	1	-	-	-	-	-	-	-	-
8	-	1	-	-	-	-	-	-	1	-
9	-	1	1	2	1	-	-	-	-	-
10	1	1	-	-	-	-	-	-	-	-
11	-	-	-	-	-	-	-	-	-	-
12	2	1	1	-	-	-	-	-	-	-
13	2	-	-	-	-	-	-	-	-	-
14	1	2	-	-	-	-	-	-	-	-
15	1	1	-	-	-	-	-	-	-	-
Total	13	14	3	2	1	0	0	0	1	0

4.3 Damage Analysis during Thawing Phase

4.3.1 Amplitude and number of hits

The number of hits per amplitude range for each specimen per cycle is shown through Tables 20 to 24. The highest amplitude for thawing was found to be 60 dB for channel 8 (specimen 4) for cycle 1. But the energy for this event was found to be low at 36 uJ, which may imply that the event was sudden and of very short duration; therefore, not much material was involved in the generation of the event. As mentioned in section 2.1, we observe during the thawing phase subsequently followed by re-freezing, the rise in temperature will result in concrete expansion which may lead to crack growth. This is the reason for having activity during thawing phase. Most number of hits are being observed in the range of <50 dB, this may be due to expansion of concrete of freezing phase.

Table 20: Number of AE hits per amplitude range during thawing phase for cylindrical specimen 1, channel 1 and 2.

Cycle	**Number of Hits per Amplitude Range (dB)**									
	< 50		**50-59**		**60-69**		**70-79**		**80 <**	
	Channel									
	1	**2**	**1**	**2**	**1**	**2**	**1**	**2**	**1**	**2**
1	1	1	-	1	-	-	-	-	-	-
2	-	-	-	-	-	-	-	-	-	-
3	-	-	-	-	-	-	-	-	-	-
4	-	-	-	-	-	-	-	-	-	-
5	-	-	-	-	-	-	-	-	-	-
6	-	-	-	-	-	-	-	-	-	-
7	-	-	1	-	-	-	-	-	-	-
8	-	-	-	-	-	-	-	-	-	-
9	-	-	-	-	-	-	-	-	-	-
10	-	-	-	-	-	-	-	-	-	-
11	-	-	-	-	-	-	-	-	-	-
12	-	-	-	-	-	-	-	-	-	-
13	-	1	-	-	-	-	-	-	-	-
14	-	-	-	-	-	-	-	-	-	-
15	-	-	-	1	-	-	-	-	-	-
Total	1	2	1	2	0	0	0	0	0	0

Table 21: Number of AE hits per amplitude range during thawing phase for cylindrical specimen 2, channel 3 and 4.

Cycle	Number of Hits per Amplitude Range (dB)									
	< 50		50-59		60-69		70-79		80 <	
	Channel									
	3	4	3	4	3	4	3	4	3	4
1	1	-	-	1	-	-	-	-	-	-
2	1	-	-	-	-	-	-	-	-	-
3	2	3	-	-	-	-	-	-	-	-
4	-	-	-	-	-	-	-	-	-	-
5	-	-	-	-	-	-	-	-	-	-
6	-	-	-	-	-	-	-	-	-	-
7	-	1	-	-	-	-	-	-	-	-
8	-	-	-	-	-	-	-	-	-	-
9	-	-	-	-	-	-	-	-	-	-
10	1	-	-	-	-	-	-	-	-	-
11	-	1	1	-	-	-	-	-	-	-
12	-	-	-	-	-	-	-	-	-	-
13	-	-	-	-	-	-	-	-	-	-
14	-	-	-	1	-	-	-	-	-	-
15	1	-	-	1	-	-	-	-	-	-
Total	6	5	1	3	0	0	0	0	0	0

Table 22: Number of AE hits per amplitude range during thawing phase for prism specimen 3, channel 5 and 6.

Cycle	Number of Hits per Amplitude Range (dB)									
	< 50		50-59		60-69		70-79		80 <	
	Channel									
	5	6	5	6	5	6	5	6	5	6
1	-	-	1	1	-	-	-	-	-	-
2	-	1	-	-	-	-	-	-	-	-
3	2	4	2	2	-	-	-	-	-	-
4	-	-	-	1	-	-	-	-	-	-
5	1	-	-	-	-	-	-	-	-	-
6	-	-	-	-	-	-	-	-	-	-
7	-	-	-	-	-	-	-	-	-	-
8	1	1	1	-	-	-	-	-	-	-
9	-	-	-	-	-	-	-	-	-	-
10	-	-	-	-	-	-	-	-	-	-
11	1	-	-	-	-	-	-	-	-	-
12	-	-	-	-	-	-	-	-	-	-
13	-	-	-	-	-	-	-	-	-	-
14	1	-	-	-	-	-	-	-	-	-
15	-	-	1	-	-	-	-	-	-	-
Total	6	6	5	4	0	0	0	0	0	0

Table 23: Number of AE hits per amplitude range during thawing phase for prism specimen 4, channel 7 and 8.

Cycle	Number of Hits per Amplitude Range (dB)									
	< 50		50-59		60-69		70-79		80 <	
	Channel									
	7	8	7	8	7	8	7	8	7	8
1	-	-	1	-	-	1	-	-	-	-
2	-	-	-	-	-	-	-	-	-	-
3	3	3	2	1	-	-	-	-	-	-
4	-	-	-	-	-	-	-	-	-	-
5	-	-	-	-	-	-	-	-	-	-
6	-	-	-	-	-	-	-	-	-	-
7	1	-	-	1	-	-	-	-	-	-
8	-	1	1	-	-	-	-	-	-	-
9	-	-	-	-	-	-	-	-	-	-
10	-	-	-	-	-	-	-	-	-	-
11	-	-	2	-	-	-	-	-	-	-
12	-	-	-	-	-	-	-	-	-	-
13	-	-	-	-	-	-	-	-	-	-
14	-	-	-	-	-	-	-	-	-	-
15	-	-	1	-	-	-	-	-	-	-
Total	4	4	7	2	0	1	0	0	0	0

4.3.2 Energy and number of hits

The number of hits per energy range for each specimen per cycle is shown through Tables 24 to 27. However, an event of larger energy was observed for prism specimen 3 where, the peak energy measured was 765 for channel 5 and channel 3. The corresponding amplitude was 50 dB. This may be because of stress-waves released by material micro cracking. The energy observed was less than that recorded during the freezing and freeze -hold phases. This indicates that the level of deterioration is not very significant during this phase. 0 – 399 uJ, is the range for the most number of hits for this phase, which low energy associated with low amplitudes as discussed above are due to expansion micro – cracks.

Table 24: Number of AE hits per energy range during thawing phase for cylindrical specimen 1, channel 1 and 2.

Cycle	Number of Hits per Energy Range									
	0-399		400-799		800-1199		1200-1600		1600 <	
	Channel									
	1	2	1	2	1	2	1	2	1	2
1	1	2	-	-	-	-	-	-	-	-
2	-	-	-	-	-	-	-	-	-	-
3	-	-	-	-	-	-	-	-	-	-
4	-	-	-	-	-	-	-	-	-	-
5	-	-	-	-	-	-	-	-	-	-
6	-	-	-	-	-	-	-	-	-	-
7	1	-	-	-	-	-	-	-	-	-
8	-	-	-	-	-	-	-	-	-	-
9	-	-	-	-	-	-	-	-	-	-
10	-	-	-	-	-	-	-	-	-	-
11	-	-	-	-	-	-	-	-	-	-
12	-	-	-	-	-	-	-	-	-	-
13	-	1	-	-	-	-	-	-	-	-
14	-	-	-	-	-	-	-	-	-	-
15	-	1	-	-	-	-	-	-	-	-
Total	2	4	0	0	0	0	0	0	0	0

Table 25: Number of AE hits per energy range during thawing phase for cylindrical specimen 2, channel 3 and 4.

Cycle	Number of Hits per Energy Range									
	0-399		400-799		800-1199		1200-1600		1600 <	
	Channel									
	3	4	3	4	3	4	3	4	3	4
1	1	1	-	-	-	-	-	-	-	-
2	1	-	-	-	-	-	-	-	-	-
3	2	2	-	1	-	-	-	-	-	-
4	-	-	-	-	-	-	-	-	-	-
5	-	-	-	-	-	-	-	-	-	-
6	-	-	-	-	-	-	-	-	-	-
7	-	1	-	-	-	-	-	-	-	-
8	-	-	-	-	-	-	-	-	-	-
9	-	-	-	-	-	-	-	-	-	-
10	1	-	-	-	-	-	-	-	-	-
11	-	1	1	-	-	-	-	-	-	-
12	-	-	-	-	-	-	-	-	-	-
13	-	-	-	-	-	-	-	-	-	-
14	-	1	-	-	-	-	-	-	-	-
15	1	1	-	-	-	-	-	-	-	-
Total	6	7	1	1	0	0	0	0	0	0

Table 26: Number of AE hits per energy range during thawing phase for prism specimen 3, channel 5 and 6.

Cycle	Number of Hits per Energy Range									
	0-399		400-799		800-1199		1200-1600		1600 <	
	Channel									
	5	6	5	6	5	6	5	6	5	6
1	1	1	-	-	-	-	-	-	-	-
2	-	1	-	-	-	-	-	-	-	-
3	1	5	3	1	-	-	-	-	-	-
4	-	1	-	-	-	-	-	-	-	-
5	1	-	-	-	-	-	-	-	-	-
6	-	-	-	-	-	-	-	-	-	-
7	-	-	-	-	-	-	-	-	-	-
8	1	-	1	1	-	-	-	-	-	-
9	-	-	-	-	-	-	-	-	-	-
10	-	-	-	-	-	-	-	-	-	-
11	1	-	-	-	-	-	-	-	-	-
12	-	-	-	-	-	-	-	-	-	-
13	-	-	-	-	-	-	-	-	-	-
14	1	-	-	-	-	-	-	-	-	-
15	1	-	-	-	-	-	-	-	-	-
Total	7	8	4	2	0	0	0	0	0	0

Table 27: Number of AE hits per energy range during thawing phase for prism specimen 4, channel 7 and 8.

Cycle	Number of Hits per Energy Range									
	0-399		400-799		800-1199		1200-1600		1600 <	
	Channel									
	7	8	7	8	7	8	7	8	7	8
1	1	1	-	-	-	-	-	-	-	-
2	-	-	-	-	-	-	-	-	-	-
3	3	3	2	1	-	-	-	-	-	-
4	-	-	-	-	-	-	-	-	-	-
5	-	-	-	-	-	-	-	-	-	-
6	-	-	-	-	-	-	-	-	-	-
7	1	1	-	-	-	-	-	-	-	-
8	-	-	1	1	-	-	-	-	-	-
9	-	-	-	-	-	-	-	-	-	-
10	-	-	-	-	-	-	-	-	-	-
11	1	-	-	-	-	-	-	-	-	-
12	-	-	-	-	-	-	-	-	-	-
13	-	-	-	-	-	-	-	-	-	-
14	-	-	-	-	-	-	-	-	-	-
15	1	-	-	-	-	-	-	-	-	-
Total	7	5	3	2	0	0	0	0	0	0

4.2 Damage Analysis during Thaw-Hold Phase

4.4.1 Amplitude and number of hits

The number of hits per energy range for each specimen per cycle is shown through Tables 28 to 31. The peak amplitude observed in this phase was 62 dB for channel 6 (specimen 3), channel 2 (specimen 1) for cycle 5 and cycle 14 respectively. The energies released were very low at this amplitudes (18 for channel 6 and 82 for channel 2). This shows there was a sudden hit at channel 5 at cycle 5, having a sudden outburst related to microcracking however not much material was involved in that process. Similarly, a minor crack have been observed for specimen 1 for cycle 14. More number of hits are observed to be in <50 amplitude range and in 0 – 399 uJ energy range, expansion of concrete causing small amount of internal friction may have been responsible for the minor events of low amplitude and low energy.

Table 28: Number of AE hits per amplitude range during thaw-hold phase for cylindrical specimen 1, channel 1 and 2.

Cycle	Number of Hits per Amplitude Range (dB)									
	< 50		50-59		60-69		70-79		80 <	
	Channel									
	1	2	1	2	1	2	1	2	1	2
1	-	-	-	-	-	-	-	-	-	-
2	-	-	-	-	-	-	-	-	-	-
3	-	-	1	-	-	-	-	-	-	-
4	-	-	-	-	-	-	-	-	-	-
5	-	1	-	-	-	-	-	-	-	-
6	-	-	-	-	-	-	-	-	-	-
7	-	-	-	-	-	-	-	-	-	-
8	-	-	-	-	-	-	-	-	-	-
9	-	-	-	-	-	-	-	-	-	-
10	-	1	-	-	-	-	-	-	-	-
11	-	-	-	-	-	-	-	-	-	-
12	-	-	-	-	-	-	-	-	-	-
13	-	1	-	-	-	-	-	-	-	-
14	-	-	-	-	-	1	-	-	-	-
15	-	-	-	-	-	-	-	-	-	-
Total	0	3	1	0	0	1	0	0	0	0

Table 29: Number of AE hits per amplitude range during thaw-hold phase for cylindrical specimen 2, channel 3 and 4.

Cycle	Number of Hits per Amplitude Range (dB)									
	< 50		50-59		60-69		70-79		80 <	
	Channel									
	3	4	3	4	3	4	3	4	3	4
1	-	1	-	-	-	-	-	-	-	-
2	-	-	-	-	-	-	-	-	-	-
3	-	-	-	-	-	-	-	-	-	-
4	-	-	-	-	-	-	-	-	-	-
5	-	-	-	-	-	-	-	-	-	-
6	-	-	-	-	-	-	-	-	-	-
7	-	-	-	-	-	-	-	-	-	-
8	-	-	-	-	-	-	-	-	-	-
9	-	-	-	-	-	-	-	-	-	-
10	1	-	1	-	-	-	-	-	-	-
11	-	-	-	-	-	-	-	-	-	-
12	-	-	-	-	-	-	-	-	-	-
13	-	-	-	1	-	-	-	-	-	-
14	-	-	-	-	-	-	-	-	-	-
15	-	-	-	-	-	-	-	-	-	-
Total	1	1	1	1	0	0	0	0	0	0

Table 30: Number of AE hits per amplitude range during thaw-hold phase for prism specimen 3, channel 5 and 6.

Cycle	Number of Hits per Amplitude Range (dB)									
	< 50		50-59		60-69		70-79		80 <	
	Channel									
	5	6	5	6	5	6	5	6	5	6
1	-	-	-	-	-	-	-	-	-	-
2	1	1	-	-	-	-	-	-	-	-
3	1	-	-	-	-	-	-	-	-	-
4	-	-	-	-	-	-	-	-	-	-
5	-	-	-	-	1	-	-	-	-	-
6	-	-	-	-	-	-	-	-	-	-
7	-	-	-	1	-	-	-	-	-	-
8	-	-	-	-	-	-	-	-	-	-
9	-	-	1	-	-	-	-	-	-	-
10	-	-	-	-	-	-	-	-	-	-
11	-	-	-	-	-	-	-	-	-	-
12	-	-	-	-	-	-	-	-	-	-
13	-	-	1	-	-	-	-	-	-	-
14	-	-	1	-	-	-	-	-	-	-
15	-	-	-	-	-	-	-	-	-	-
Total	2	1	3	1	1	0	0	0	0	0

Table 31: Number of AE hits per amplitude range during thaw-hold phase for prism specimen 4, channel 7 and 8.

Cycle	Number of Hits per Amplitude Range (dB)									
	< 50		50-59		60-69		70-79		80 <	
	Channel									
	7	8	7	8	7	8	7	8	7	8
1	-	-	-	-	-	1	-	-	-	-
2	-	-	-	-	-	-	-	-	-	-
3	1	-	-	-	-	-	-	-	-	-
4	-	1	-	-	-	-	-	-	-	-
5	1	1	-	-	-	-	-	-	-	-
6	-	-	-	-	-	-	-	-	-	-
7	1	0	-	-	-	-	-	-	-	-
8	-	-	-	-	-	-	-	-	-	-
9	1	-	-	-	-	-	-	-	-	-
10	1	-	2	-	-	-	-	-	-	-
11	-	-	-	-	-	-	-	-	-	-
12	-	1	-	-	-	-	-	-	-	-
13	-	-	-	-	-	-	-	-	-	-
14	-	-	-	-	-	-	-	-	-	-
15	-	-	-	-	-	-	-	-	-	-
Total	5	3	2	0	0	1	0	0	0	0

4.4.2 Energy and number of hits

The number of hits per energy range for each specimen per cycle is shown through Tables 32 to35. The peak energy observed was 10354 for channel 8 (specimen 4), cycle 5. The corresponding amplitude was 45 dB. Again, the higher energy may indicate the localized failure of the material as expressed previously.

Table 32: Number of AE hits per energy range during thaw-hold phase for cylindrical specimen 1, channel 1 and 2.

Cycle	Number of Hits per Energy Range									
	0-399		400-799		800-1199		1200-1600		1600 <	
	Channel									
	1	2	1	2	1	2	1	2	1	2
1	-	-	-	-	-	-	-	-	-	-
2	-	-	-	-	-	-	-	-	-	-
3	1	-	-	-	-	-	-	-	-	-
4	-	-	-	-	-	-	-	-	-	-
5	-	1	-	-	-	-	-	-	-	-
6	-	-	-	-	-	-	-	-	-	-
7	-	-	-	-	-	-	-	-	-	-
8	-	-	-	-	-	-	-	-	-	-
9	-	-	-	-	-	-	-	-	-	-
10	-	1	-	-	-	-	-	-	-	-
11	-	-	-	-	-	-	-	-	-	-
12	-	-	-	-	-	-	-	-	-	-
13	-	1	-	-	-	-	-	-	-	-
14	-	1	-	-	-	-	-	-	-	-
15	-	-	-	-	-	-	-	-	-	-
Total	1	4	0	0	0	0	0	0	0	0

Table 33: Number of AE hits per energy range during thaw-hold phase for cylindrical specimen 2, channel 3 and 4.

Cycle	Number of Hits per Energy Range									
	0-399		400-799		800-1199		1200-1600		1600 <	
	Channel									
	3	4	3	4	3	4	3	4	3	4
1	-	-	-	-	-	-	-	-	-	-
2	-	1	-	-	-	-	-	-	-	-
3	-	-	-	-	-	-	-	-	-	-
4	-	-	-	-	-	-	-	-	-	-
5	-	-	-	-	-	-	-	-	-	-
6	-	-	-	-	-	-	-	-	-	-
7	-	-	-	-	-	-	-	-	-	-
8	-	-	-	-	-	-	-	-	-	-
9	-	-	-	-	-	-	-	-	-	-
10	2	-	-	-	-	-	-	-	-	-
11	-	-	-	-	-	-	-	-	-	-
12	-	-	-	-	-	-	-	-	-	-
13	-	1	-	-	-	-	-	-	-	-
14	-	-	-	-	-	-	-	-	-	-
15	-	-	-	-	-	-	-	-	-	-
Total	2	2	0	0	0	0	0	0	0	0

Table 34: Number of AE hits per energy range during thaw-hold phase for prism specimen 3, channel 5 and 6.

Cycle	Number of Hits per Energy Range									
	0-399		400-799		800-1199		1200-1600		1600 <	
	Channel									
	5	6	5	6	5	6	5	6	5	6
1	-	-	-	-	-	-	-	-	-	-
2	1	1	-	-	-	-	-	-	-	-
3	1	-	-	-	-	-	-	-	-	-
4	-	-	-	-	-	-	-	-	-	-
5	-	1	-	-	-	-	-	-	-	-
6	-	-	-	-	-	-	-	-	-	-
7	-	1	-	-	-	-	-	-	-	-
8	-	-	-	-	-	-	-	-	-	-
9	1	-	-	-	-	-	-	-	-	-
10	-	-	-	-	-	-	-	-	-	-
11	-	-	-	-	-	-	-	-	-	-
12	-	-	-	-	-	-	-	-	-	-
13	1	-	-	-	-	-	-	-	-	-
14	1	-	-	-	-	-	-	-	-	-
15	-	-	-	-	-	-	-	-	-	-
Total	5	3	0	0	0	0	0	0	0	0

Table 35: Number of AE hits per energy range during thaw-hold phase for prism specimen 4, channel 7 and 8.

Cycle	Number of Hits per Energy Range									
	0-399		400-799		800-1199		1200-1600		1600 <	
	Channel									
	7	8	7	8	7	8	7	8	7	8
1	-	1	-	-	-	-	-	-	-	-
2	-	-	-	-	-	-	-	-	-	-
3	1	-	-	-	-	-	-	-	-	-
4	-	1	-	-	-	-	-	-	-	-
5	1	-	-	-	-	-	-	-	-	1
6	-	-	-	-	-	-	-	-	-	-
7	1	-	-	-	-	-	-	-	-	-
8	-	-	-	-	-	-	-	-	-	-
9	1	-	-	-	-	-	-	-	-	-
10	3	-	-	-	-	-	-	-	-	-
11	-	-	-	-	-	-	-	-	-	-
12	-	-	-	-	-	-	-	-	-	1
13	-	-	-	-	-	-	-	-	-	-
14	-	-	-	-	-	-	-	-	-	-
15	-	-	-	-	-	-	-	-	-	-
Total	7	2	0	0	0	0	0	0	0	2

CHAPTER 5

CONCLUSION

As the concrete specimen is subjected to freezing and thawing micro-cracks initiate within the concrete. At this point, a small amount of energy is released which causes a stress pulse to be initiated. Most of the hits for both amplitude and energy for freezing phase, thawing phase and thaw – hold phase are observed to be in the range of < 50 dB and 0 – 399 uJ respectively (Chapter 4). This low amplitude and low energy may be observed due to microcracking of concrete. The above mentioned phases were maintained for 6 hours each, except for freeze-hold which was maintained for 12 hours. The cumulative number of hits for all the channels are:

- Freezing phase was - 59
- Freeze - hold phase was - 101
- Thawing phase - 60
- Thaw - hold phase – 28

The low number of hits recorded may be due to initiation of micro racks. This may be because the relative humidity of the samples were maintained at approximately 60% during the exposure period which may be lower than the critical saturation point causing damage. As previously demonstrated in past investigations, most of the AE events are observed to be at the freezing and freezing hold phase which could be due to the water freezing in the voids and capillary pores. Most of the amplitudes and energies recorded were low thus, significant damage may not have occurred.

REFERENCES

A. Carpinteri, G. Lacidogna, N. Pugno (2007). "Structural damage diagnosis and life-time assessment by acoustic emission monitoring," Engineering Fracture Mechanics, 74, 273-289.

A.M. Veville (1996). Properties of Concrete: Effects of feezing and thawing and of chlorides, John Wiley & Sons, Inc. New York, NY,

ACI 201.2R-92, Guide to durable concrete, ACI Manual of Concrete Practice, Part I: Materials and General Properties of Concrete, 41 pp. (Detroit, Michigan, 1994)

Aggelis, D. G., A.C. Mpalaskas b, T.E. Matikas (2013). "Investigation of different fracture modes in cement-based materials by acoustic emission". Cement and Concrete Research, 48, 1–8.

ASTM C 138/C 138M (2014). "Standard Test Method for Density (Unit Weight), Yield, and Air Content (Gravimetric) of Concrete." ASTM International.

ASTM C 143 / C 143 M (2008). "Standard Test Method for Slump of Hydraulic-Cement Concrete." ASTM International.

ASTM C 150/C 150M (2012). "Standard Specification for Portland Cement." ASTM International

ASTM C 172 (2008). "Standard Practice for Sampling Freshly Mixed Concrete." ASTM International

ASTM C 192 (2008). "Standard Practice for Making and Curing Concrete Test Specimens in the Laboratory." ASTM International

ASTM C 231 (2010). “Standard Test Method for Air Content of Freshly Mixed Concrete by the Pressure Method.” ASTM International

ASTM C 33 (2012). “Standard Specification for Concrete Aggregates.” ASTM International

ASTM C 39/C 39M (2004). “Standard Test Method for Compressive Strength of Cylindrical Concrete Specimens.” ASTM International

ASTM C 470 (2009). “Standard Specification for Molds for Forming Concrete Test Cylinders Vertically.” ASTM International

ASTM C 597 – 97 (2009). “Standard Test Method forPulse Velocity through Concrete.” ASTM International

ASTM C 618 (2012). “Standard Specification for Coal Fly Ash and Raw or Calcined Natural Pozzolana for Use in Concrete.” ASTM International

ASTM C 642 (2004). “Standard Test Method for Density, Absorption, and Voids in Hardened Concrete.” ASTM International

ASTM C 666/C 666M (2003). “Standard Test Method for Resistance of Concrete to Rapid Freezing and Thawing.” ASTM International

ASTM C 685/C 685M (2012) “Standard Specification for Concrete Made by Volumetric Batching and Continuous Mixing.” ASTM International

ASTM C 78 (2009). “Standard Test Method for Flexural Strength of Concrete (Using Simple Beam with Third-Point Loading.” ASTM International

Braile. L. (2010). “Seismic Waves and the Slinky: A guide for Teachers”. Web.ics.perdue.edu. <http://web.ics.purdue.edu/~braile/edumod/slinky/slinky.htm>

Carino, N.J. (1997). “Nondestructive Test Methods” in Concrete Construction Engineering Handbook, E.G. Nawy (ed), CRC Press, Boca Raton, Fl, 19/1-68 pp.

D.W. Pfeifer, W.F. Perenchio and W.G. Hime (1992). “A critique of the ACI 318 chloride limits.” PCI Journal, 37, 5, 68-71.

D.W.S. Ho and R.K. Lewis (1988). “The specification of concrete for reinforcement protection – performance criteria and compliance by strength.” Cement and Concrete Research, 18, 4, 584-94.

Ye Qian, YaghoobFarnam and Jason Weiss (2014), “Using Acoustic Emission to Quantify Freeze-Thaw Damage of Mortar Saturated with NaCl Solutions”, Purdue University.

Mehta PK, Monteiro PJM. “Concrete: microstructure, properties, and materials.” 3rd ed. McGraw-Hill; 2006

Mistras Group Inc. (2011). “Principles and Techniques of Acoustic Emission”. AE Level II Course Notebook

Eruption. “The electronic field trip.” <http://electronicfieldtrip.org/volcanoes/teachers/classroom_causes.html>. (June 15, 2015)

Setzer MJ (2001). “Micro-ice-lens formation in porous solid.” J Colloid Interface Sci, 243, 193–201.

G.J. Verbeck and P. Kleiger (1958). “Calorimeter-strain apparatus for study of freezing and thawing concrete.” Highw. Res. Bd Bull, 176, 9-12.

H. Cai and X. Liu (1998). “Freeze-thaw durability of concrete: Ice formation process in pores.” Elsevier, Cement and Concrete Research, 28, 9, 1281–1287.

Huaishuai Shang, Yupu Song, Jinping Ou (2009). “Behavior of Air-Entrained Concrete after Freeze-Thaw Cycles.” Acta Mechanica Solida Sinica, 22, 3, ISSN 0894-9166.

Huang, Miinshiou, Liang Jiang, Peter K. Liaw, Charlie R. Brooks, Rodger Seeley, and Dwaine L. Klarstrom (1998). “Using Acoustic Emission in Fatigue and Fracture Materials Research”. JOM-e, 50, 11.

M. Molero, S. Aparicio, G. Al-Assadi, M.J. Casati, M.G.Hernandez, J.J. Anaya (2012). “Evaluation of freeze–thaw damage in concrete by ultrasonic imaging.” Elsevier, NDT&E International, 52, 86–94.

M. Molero, S. Aparicio, G. Al-Assadi, M.J. Casati, M.G.Hernandez, J.J. Anaya (2012). “Evaluation of freeze–thaw damage in concrete by ultrasonic imaging.” Elsevier, NDT&E International, 52, 86–94.

Naik, Tarun R., V. Mohan Malhotra, John S. Popovics (2004). “The Ultrasonic Pulse Velocity Method” in Handbook on Nondestructive Testing of Concrete, 2nd ed. N.J. Carino and V.M. Malhotra Eds., CRC Press, 4/19 p

Ohtsu, M., Uchida, M., Okamoto, T. and Yuyama, S. (2002),”Damage Assessment of Reinforced Concrete Beams qualified by AE.” ACI Structural Journal, 99, 4, 411-417.

P. Schiessl and N. Raupach (1989). “Influence of blending agents on the rate of corrosion of steel in concrete, in Durability of Concrete: Aspects of admixtures and Industrial By-products.” 2nd International Seminar, Swedish Council for Building Research, 205-14.

Pollock, A. A (1989). "Acoustic Emission Inspection." Metals Handbook, 17, 278-294.

Power TC (1958). “The physical structure and engineering properties of concrete.” Bulletin 90. Skokie, IL: Portland cement Association.

Powers TC, Helmuth RA (1953). “Theory of volume changes in hardened Portland cement paste during freezing.” Highw Res Board Bull, 32, 285–97

Shahiron Shahidan, Rhys Pulin, Norazura Muhamad Bunnori, Karen M. Holford (2013). "Damage classification in reinforced concrete beam by acoustic emission signal analysis." Construction and Building Materials, 45, 78–86

Shang Huai-shuai, Song Yu-pu (2008). "Behavior of air-entrained concrete under the compression with constant confined stress after freeze–thaw cycles." Elsevier, Cement & Concrete Composites, 30, 854–860

T. Uomoto (Ed.) (2000). Non-Destructive Testing in Civil Engineering, Elsevier, Amsterdam.

T.C. Powers (1955), "Basic consideration pertaining to freezing and thawing tests." Proc. ASTM 55, 1132-54.

U.S Climate Data. "Temperature". <http://www.usclimatedata.com/> (Jan. 10, 2015)

V.M. Malhotra, N.J. Carino (Eds.) (1991.), CRC Handbook on Nondestructive Testing of Concrete, CRC Press, Florida.

Won-Chang Choi, Hyun-Do Yun (2015). "Acoustic emission activity of CFRP-strengthened reinforced concrete beams after freeze–thaw cycling." Elsevier, Cold Regions Science and Technology, 110, 47–58.

Y. Farnam, D. Bentz, A. Hampton, and J. Weiss (2013). "Acoustic Emission and Low Temperature Calorimetry Study of Freeze and Thaw Behavior in Cementitious Materials Exposed to NaCl Salt. Purdue University.

Yuyama, S, Z.-W. Li, M. Yoshizawa, T. Tomokiyo, T. Uomoto (2001). "Evaluation of fatigue damage in reinforced concrete slab by acoustic emission." NDT&E International, 34, 381-387.

Yuyama, S., Okamoto, T., Shigeishi, T., Ohtsu, M. and Kishi, T. (1999). “A Proposed Standard for Evaluating Structural Integrity of Reinforced Concrete Beams by AE.” Acoustic Emission: Standards and Technology Update. ASTM STP 1353, 25-40.

APPENDICES

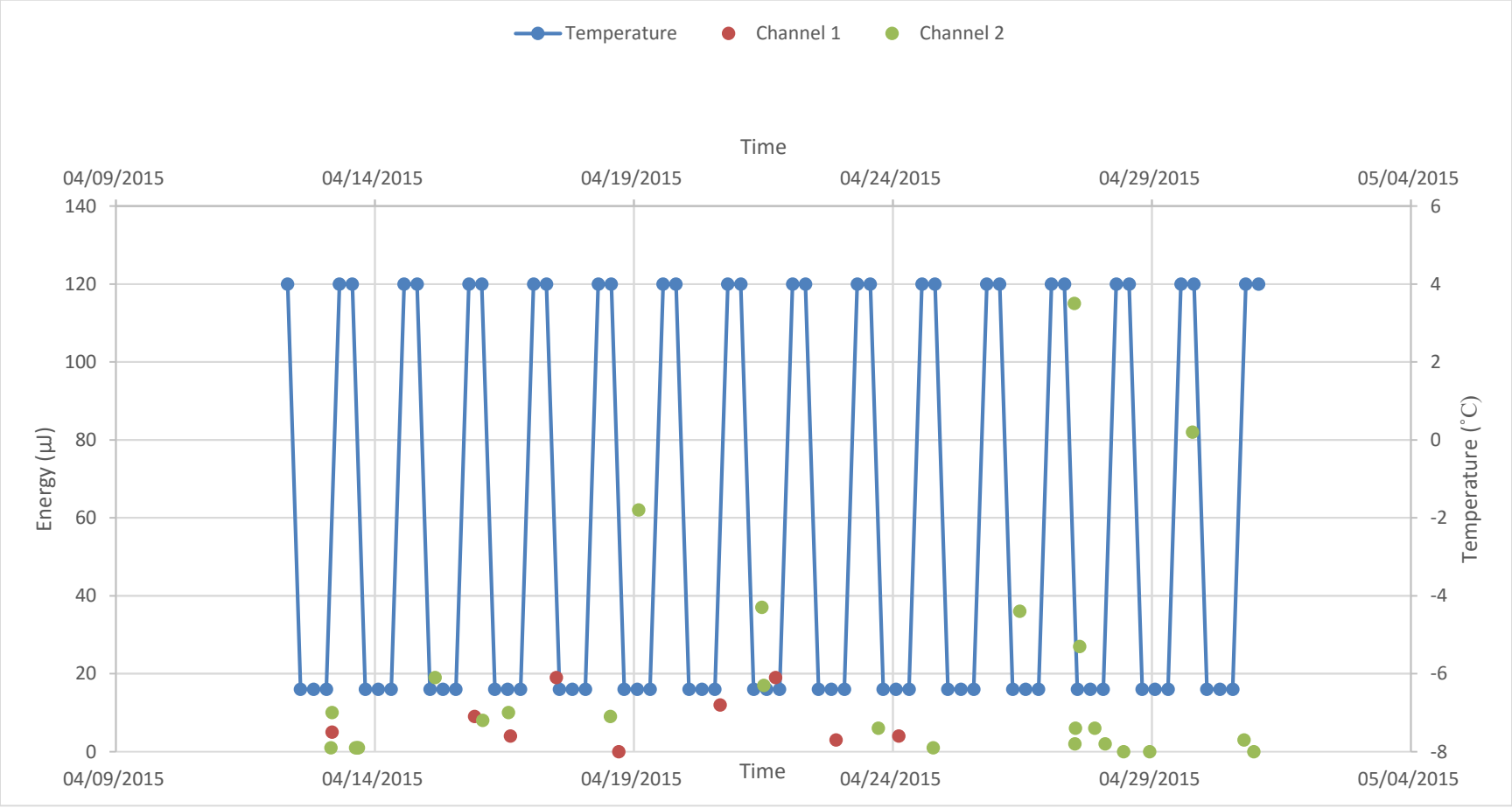

Figure 11: Temperature vs Energy graph for channel 1 and 2 (cylindrical specimen 1)

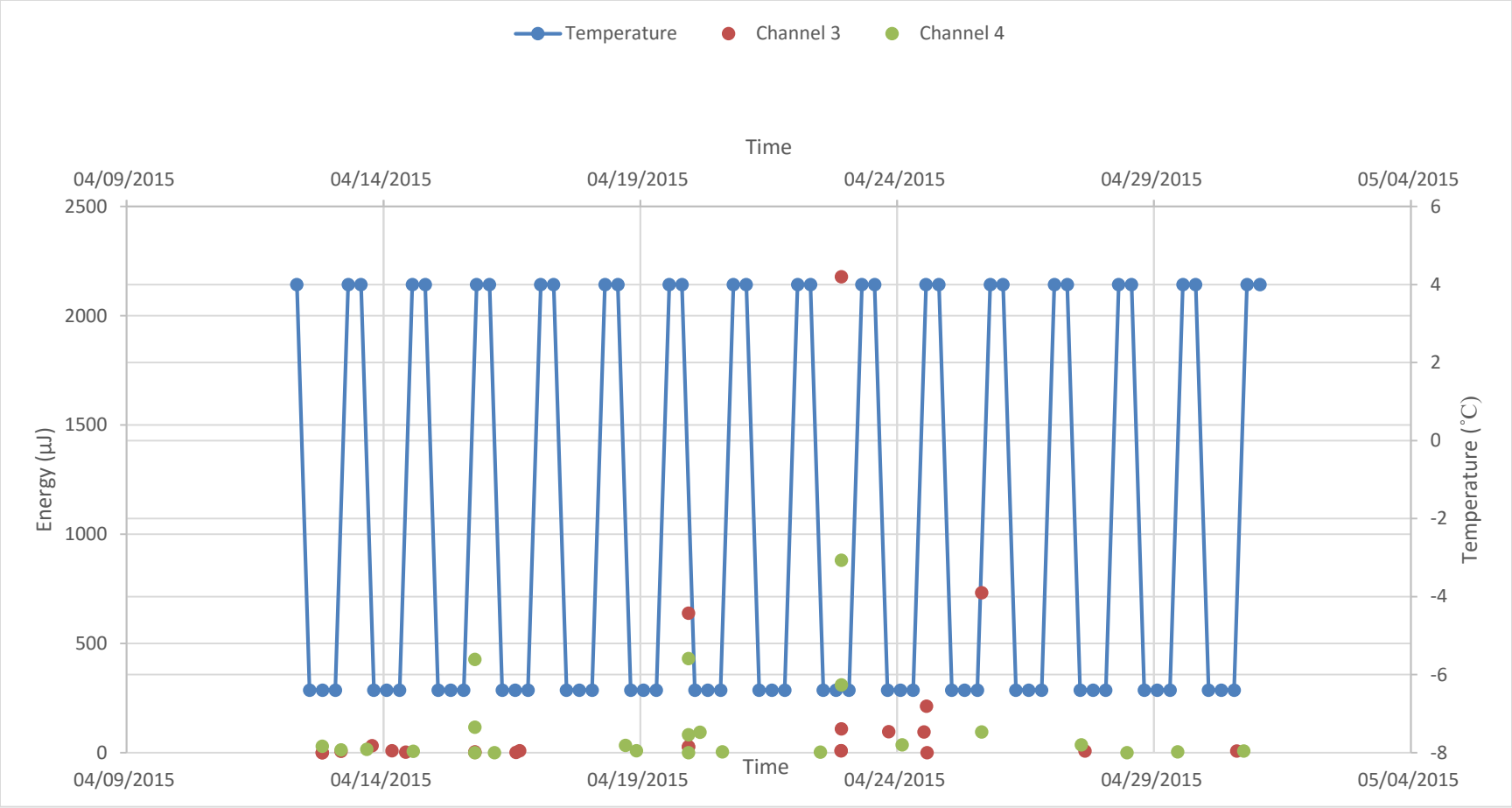

Figure 12: Temperature vs Energy graph for channel 3 and 4 (cylindrical specimen 2)

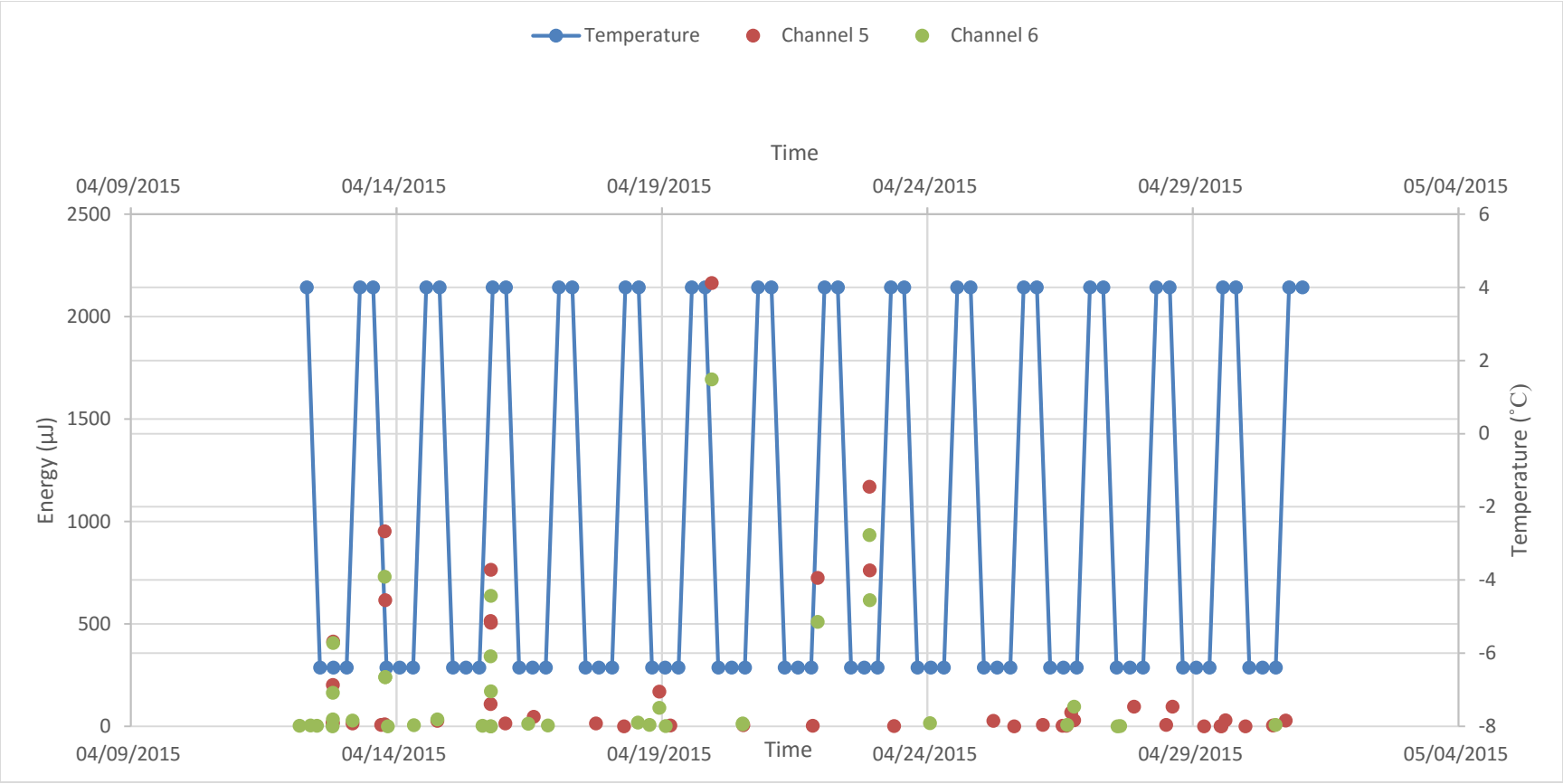

Figure 13: Temperature vs Energy graph for channel 5 and 6 (prism specimen 3)

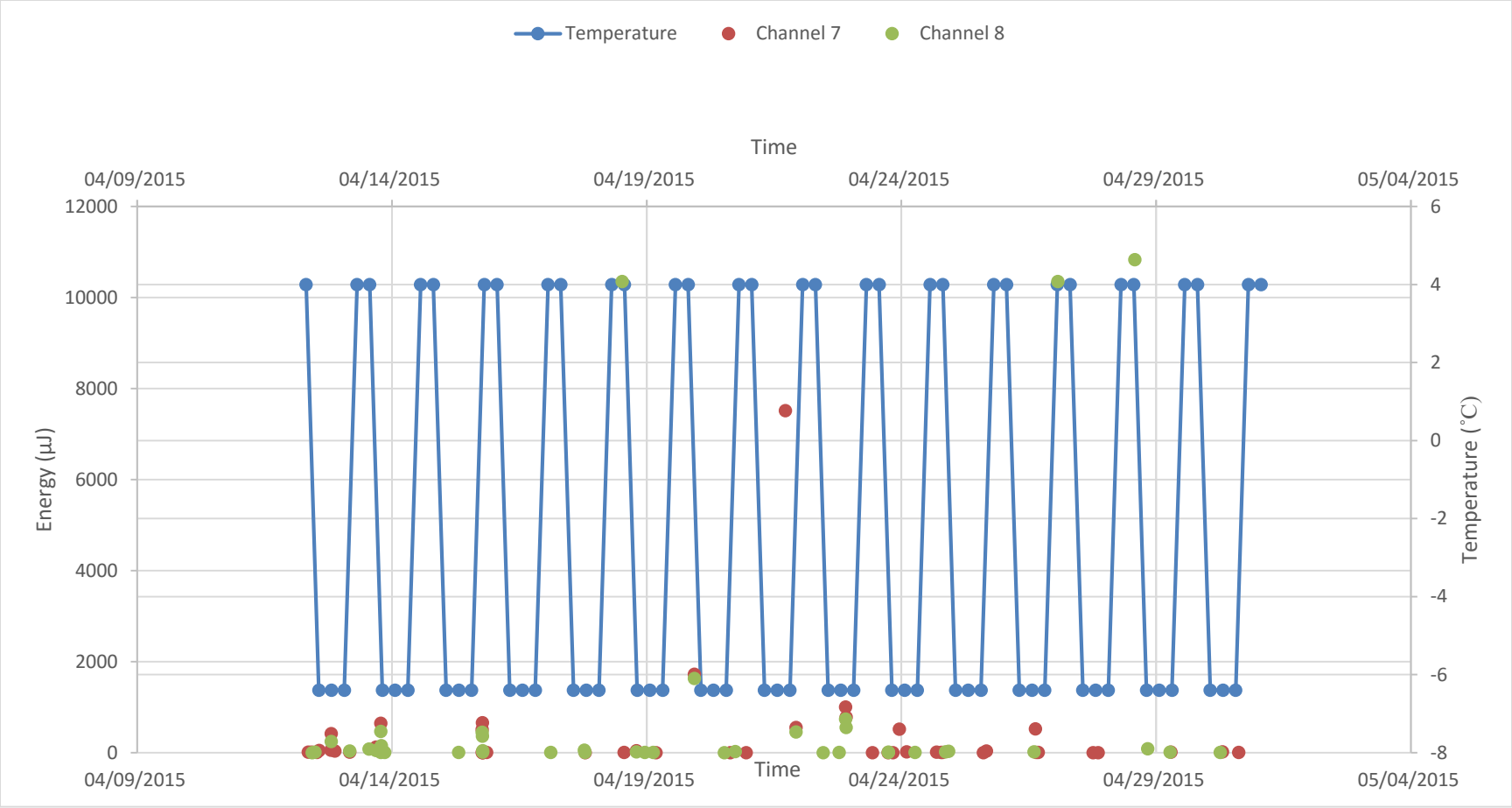

Figure 14: Temperature vs Energy graph for channel 7 and 8 (prism specimen 4)

Figure 15: Temperature vs Amplitude graph for channel 1 and 2 (cylindrical specimen 1)

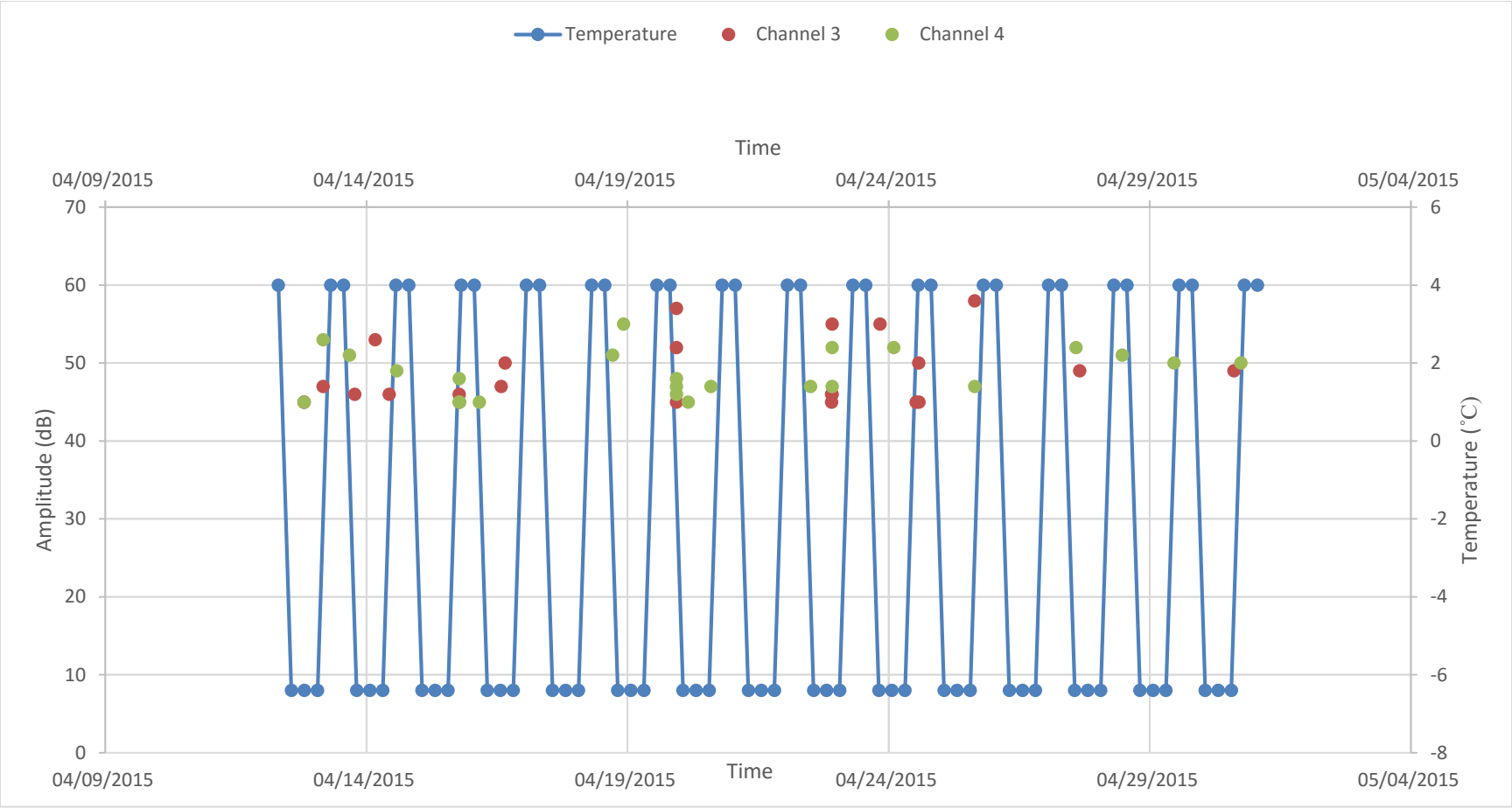

Figure 16: Temperature vs Amplitude graph for channel 3 and 4 (cylindrical specimen 2)

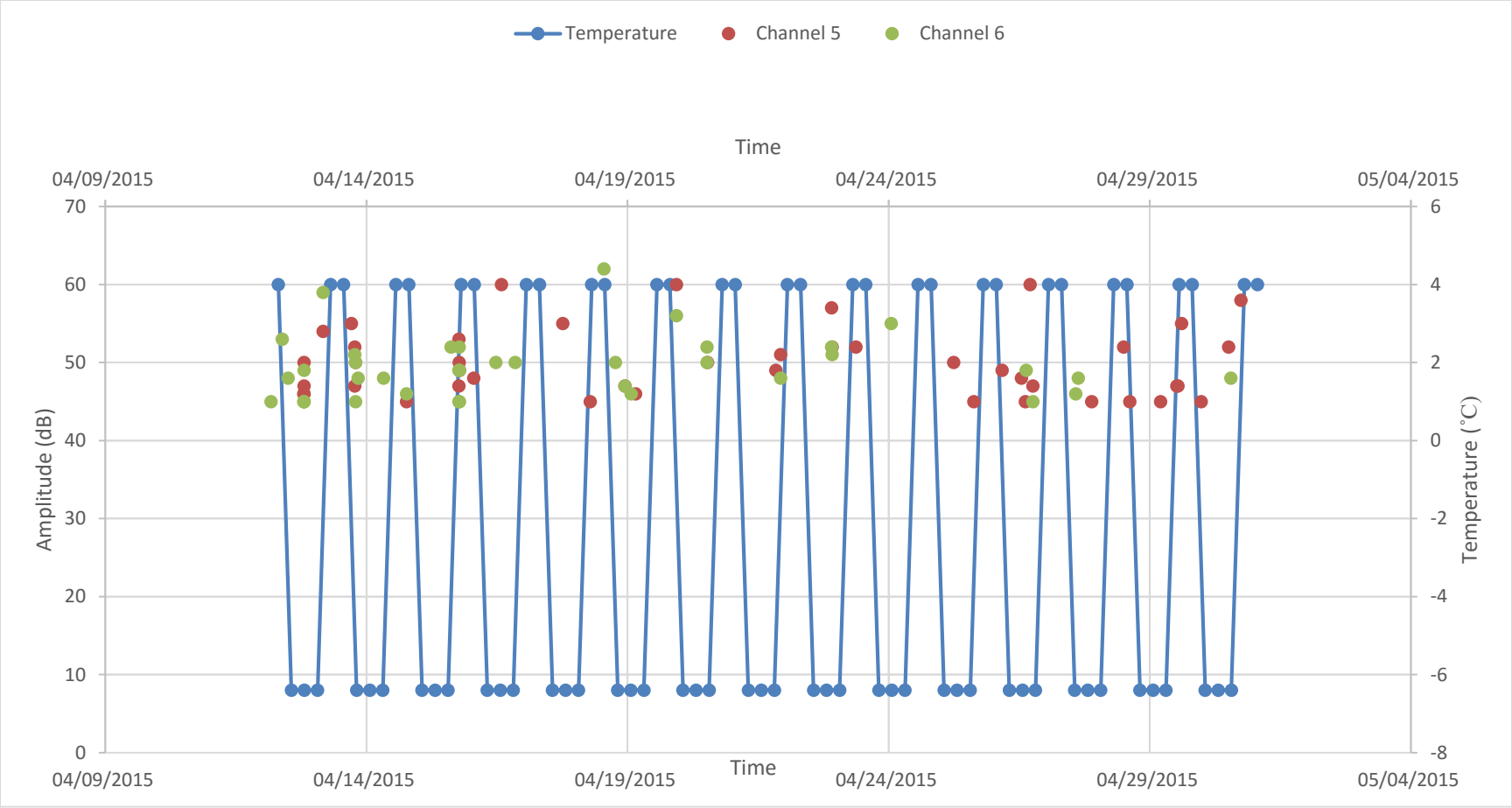

Figure 17: Temperature vs Amplitude graph for channel 5 and 6 (prism specimen 3)

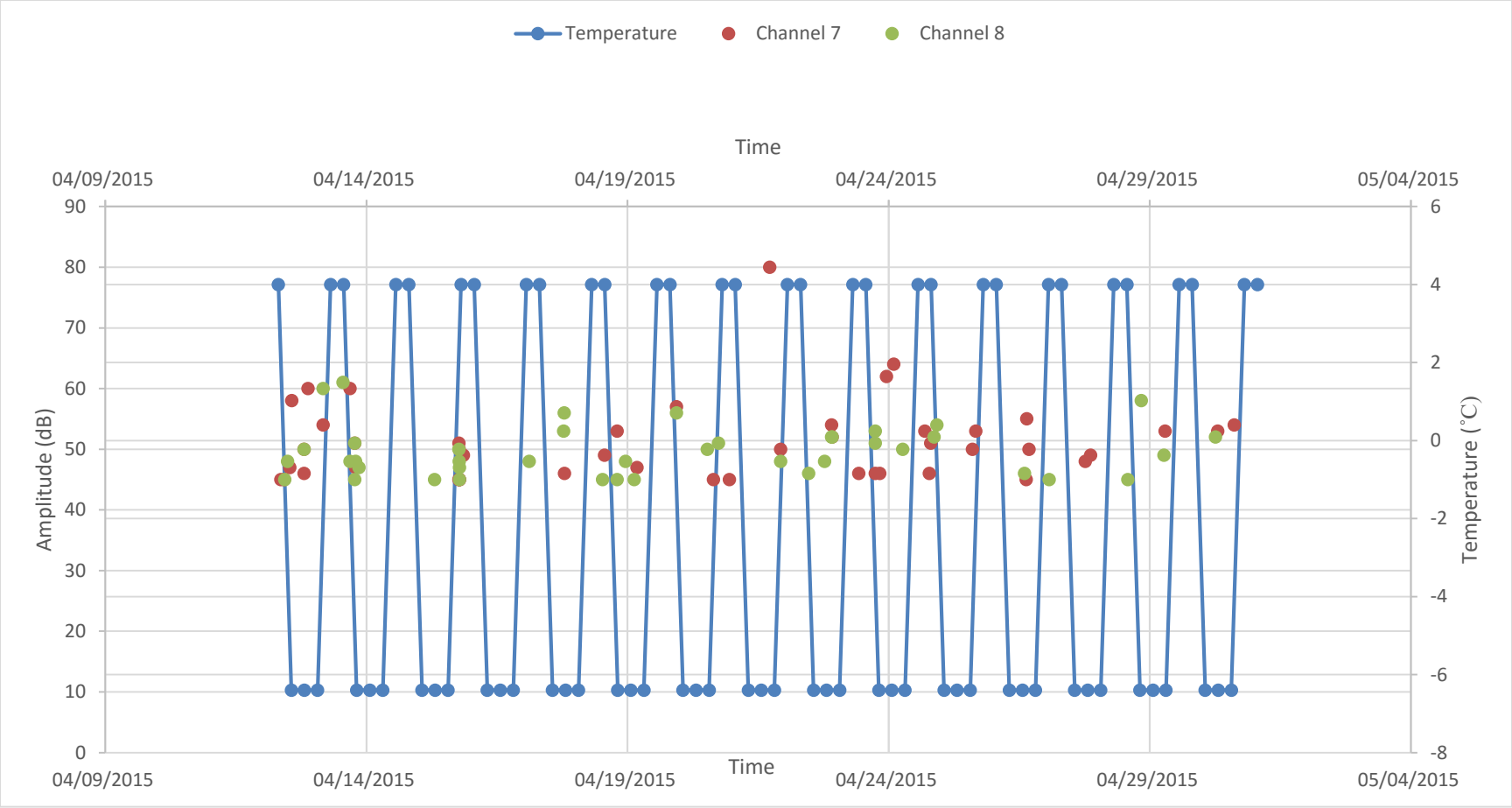

Figure 18: Temperature vs Amplitude graph for channel 7 and 8 (prism specimen 4)

VITA

Ignatius Vasant

Candidate for the Degree of

Master of Science

Thesis: INVESTIGATING EFFECTS OF TEMPERATURE CHANGE ON CONCRETE USING ACOUSTIC EMISSION MONITORING

Major Field: Civil Engineering

Biographical:

Education:

Completed the requirements for the Master of Science in Civil Engineering at Oklahoma State University, Stillwater, Oklahoma in July, 2015.

Completed the requirements for the Bachelor of Engineering in Civil Engineering at Visvesvaraya Technological University, Belgaum, Karnataka/India in 2013.